International Communications in Heat and Mass Transfer 164 (2025) 108929

Contents lists available at ScienceDirect

International Communications in Heat and Mass Transfer

journal homepage: www.elsevier.com/locate/ichmt

# Flow boiling heat transfer of new refrigerant blends: Experimental data in a microchannel and modelling

Nicolò Mattiuzzo, Marco Azzolin, Arianna Berto *, Stefano Bortolin, Davide Del Col

*Department of Industrial Engineering, University of Padova, Via Venezia 1, 35131 Padova, Italy*

ARTICLE INFO

*Keywords:*
Flow boiling
Heat transfer coefficient
R513A
R516A
R515B
R450A

ABSTRACT

Mixtures of hydrofluorocarbons (HFCs) and hydrofluoroolefins (HFOs) are suitable as drop-in substitutes in refrigeration and air conditioning, due to the low global warming potential (GWP) and desired thermodynamic properties. In the present work, the flow boiling heat transfer of four HFOs/HFCs mixtures has been studied inside a 0.96 mm diameter channel. Three of those mixtures, R513A (R1234yf/R134a, 56/44 % by mass, $GWP_{100\text{-}y}$ = 629), R516A (R1234yf/R152a/R134a 77.5/14/8.5 % by mass, $GWP_{100\text{-}y}$ = 131) and R515B (R1234ze(E)/R227ea, 91/9 % by mass, $GWP_{100\text{-}y}$ = 299), are azeotropic mixtures, while the fourth is quasi-azeotropic mixture R450A (R1234ze(E)/R134a, 56/44 % by mass, $GWP_{100\text{-}y}$ = 547, $\Delta T_{GL}$ = 0.63 K at 30 °C). The experimental campaign was conducted using a test section where the flow boiling is promoted by a secondary fluid, at 30 °C mean saturation temperature and mass flux between 300 kg $m^{-2}$ $s^{-1}$ and 600 kg $m^{-2}$ $s^{-1}$. The present data have been compared with the heat transfer coefficient of R134a, in order to assess the suitability of its drop-in substitutes. From the comparison between experimental data and the predictions from some semi-empirical models, a modified method is presented. The new flow boiling heat transfer correlation has been successfully tested with data of propane, propylene, R32 and R1234yf.

## 1. Introduction

Over recent years increased attention has been reserved to environmental impact related to all human activities, leading to the introduction of new regulations and consequently restrictions in many sectors, from transportation to civil applications. Among all the affected sectors, refrigeration for civil and industrial applications has been regulated with the EU regulation 573/2024 in which the European Union sets the hydrofluorocarbons (HFCs) phase-out, including R134a ($GWP_{100\text{-}y}$ = 1300 according to [1]). In particular, refrigerants having global warming potential higher than 150 will be progressively banned, with this limitation becoming effective from 2027. However, the employment of refrigerants with GWP higher than 150 but lower than 750 will still be allowed in mono-split air conditioning and heat pump systems. The first proposed solutions for the substitution of R134a were hydrofluoroolefins (HFOs), such as R1234yf and R1234ze(E). The $GWP_{100\text{-}y}$ of most HFOs is lower than 2 [1] and they are classified as mildly flammable A2L [2]. The reliability of HFOs as substitutes of R134a has been investigated by many studies, regarding both the comparison of the two-phase heat transfer performance of HFOs and R134a and the comparative analysis operation of existing systems with the hydrofluoroolefins and the HFC. Del Col et al. [3,4] experimentally studied both condensation of R1234yf and R1234ze(E) and flow boiling of R1234yf and compared the results with R134a. In their work, the authors concluded that there was no significant difference between the flow boiling HTC of R1234yf and R134a. Moreover, Diani et al. [5,6] measured the experimental flow boiling HTCs of R1234yf and R1234ze (E) inside a 3.4 mm ID microfin tube and compared the experimental heat transfer coefficient of the hydrofluoroolefins and R134a. The authors find out that the flow boiling heat transfer coefficients of R1234yf are slightly lower than those of R134a at high vapor quality, but comparable at low vapor quality values, while R1234ze(E) HTCs are from 8 % to 10 % lower than the flow boiling heat transfer coefficient of R134a. Regarding the investigation of the drop-in substitution of R134a in existing refrigerant systems, Li et al. [7] experimentally compared the replacement of the HFC with R1234yf in an oil-free VCR system, highlighting that with the hydrofluoroolefin the COP is from 5 % to 20 % lower.

In searching for possible drop-in substitutes for R134a, mixtures of HFC and HFO have gained more and more interest since they have low GWP values. These mixtures generally display GWP higher than 150 but

* Corresponding author.
*E-mail address:* arianna.berto@unipd.it (A. Berto).

https://doi.org/10.1016/j.icheatmasstransfer.2025.108929

**Nomenclature**

| | |
|---|---|
| $B$ | Scaling factor [/] |
| $c$ | Specific heat [J kg$^{-1}$ K$^{-1}$] |
| COP | Coefficient of Performance [/] |
| $d$ | Diameter [m] |
| $E$ | Enhancement factor of the convective boiling [/] |
| $e_R$ | Mean percentage error [%], $= (1/N_p)\sum[(\alpha_{calc}-\alpha_{meas})/\alpha_{meas}]\cdot 100$ |
| $e_{AB}$ | Mean absolute percentage error [%], $= (1/N_p)\sum(\lvert\alpha_{calc}-\alpha_{meas}\rvert/\alpha_{meas})\cdot 100$ |
| $F_c$ | Mixture correction factor [/] |
| $G$ | Mass flux [kg m$^{-2}$ s$^{-1}$] |
| $GWP_{100\text{-}y}$ | Global Warming Potential over 100 years [/] |
| $h$ | Specific enthalpy [J kg$^{-1}$] |
| $h_{LG}$ | Latent heat [J kg$^{-1}$] |
| HTC | Heat transfer coefficient [W m$^{-2}$ K$^{-1}$] |
| $K$ | Coverage factor [/] |
| $\dot{m}$ | Mass flow rate [kg s$^{-1}$] |
| $M$ | Molecular mass [kg kmol$^{-1}$] |
| $N_p$ | Number of experimental data points [/] |
| $p$ | Pressure [bar] |
| $p_r$ | Reduced pressure [/], $= (p/p_{crit})$ |
| $q'$ | Heat flux [W m$^{-2}$] |
| $Ra$ | Inner surface roughness according to ISO 4287 [μm] |
| $Rp$ | Roughness according to DIN 4762/1 [μm] |
| $S$ | Suppression factor of the nucleate boiling [/] |
| $T$ | Temperature [°C] |
| $T_{dew}$ | Dew-point emperature [°C] |
| $U_\alpha$ | Heat transfer coefficient standard expanded uncertainty [%] |
| $U_{q'}$ | Heat flux standard expanded uncertainty [%] |
| $U_x$ | Vapor quality standard expanded uncertainty [/] |
| $x$ | Thermodynamic vapor quality [/] |
| $z$ | Axial position [m] |

*Greek letters*

| | |
|---|---|
| $\alpha(z)$ | Local heat transfer coefficient, HTC [W m$^{-2}$ K$^{-1}$] |
| $\alpha_f$ | Heat transfer coefficient calculated with a general correlation [W m$^{-2}$ K$^{-1}$] |
| $\beta_L$ | Liquid mass transfer coefficient [/] |
| $\rho$ | Density [kg m$^{-3}$] |
| $\mu$ | Dynamic viscosity [kg m$^{-1}$ s$^{-1}$] |
| $\Delta h_m$ | Isobaric enthalpy change of the mixture [J kg$^{-1}$] |
| $\Delta T_{GL}$ | Mixture temperature glide [K] |
| $\lambda$ | Thermal conductivity [W m$^{-1}$ K$^{-1}$] |
| $\sigma$ | Surface tension [mN m$^{-1}$] |
| $\sigma_N$ | Standard deviation [%], $= \left\{\left[\sum(e-e_R)^2\right]/(N_p-1)\right\}^{1/2}\cdot 100$ |

*Subscripts*

| | |
|---|---|
| *cb* | Convective boiling |
| *IN* | Inlet |
| *L* | Liquid |
| *m* | Mixture |
| *nb* | Nucleate boiling |
| *OUT* | Outlet |
| *r* | Refrigerant |
| *sat* | Saturation |
| *V* | Vapor |
| *wat* | Water |
| *wall* | Wall |

significantly lower than pure HFCs. However, their GWP is largely below 750, thus still in the allowed range. Several researchers investigated the possibility of a drop-in substitution of hydrofluorocarbons with HFC/HFO mixtures [8–11]. Focusing on the replacement of R134a, Mateu-Rojo et al. [12] tested R1234ze(E) and R515B (R1234ze(E)/R227ea, 91/9 % by mass) in a medium and moderately high heat pump designed for R134a. The experimental analysis pointed out that R515B presents a considerably high performance, especially for the higher temperature and that the COPs of the mixture are similar to those of R134a. Makhnatch et al. [13] conducted an experimental campaign with R450A (R1234ze(E)/R134a 58/42 % by mass) and R513A (R1234yf/R134a 56/44 % by mass) inside a small refrigeration system for high ambient temperature countries. Comparing the obtained COP with the performances of the refrigeration systems with R134a, they observed that R513A presents the highest COP while there was a 5.3 % reduction in the COP using R450A. Finally, Al-Sayyab et al. [14] tested a vapor compression cooling and heating system operating with R1234yf, R513A and R516A. While R516A was found to be more suitable for low evaporation temperatures, it was found that the highest COP were reached by R513A.

While some works regarding the deployment of R513A, R516A, R515B and R450A in refrigerating systems and heat pumps were found in the literature, very limited studies regard the flow boiling of these mixtures. Considering the flow boiling inside circular channels, Diani et al. [15] evaluated the flow boiling of R513A inside a horizontal smooth tube microfin tube, while Kedzierski et al. [16] studied the convective boiling of R450A inside a horizontal microfin tube. Instead, to the best of the author's knowledge there are no studies that investigate the flow boiling heat transfer of R516A and R515B inside tubes. Moreover, the flow boiling models used to predict the heat transfer coefficient are often unable to give a prediction in good agreement with the experiments. In fact, in [4,17,18] the authors reported an average deviation of more than 25 % with the majority of the models.

Thus, it is of utmost importance to obtain experimental data on new mixtures to assess existing correlations. To address this gap, the present paper experimentally investigates the flow boiling heat transfer of HFC/HFO mixtures R513A, R516A, R515B, and R450A inside a minichannel with an internal diameter of 0.96 mm. Research on these fluids is crucial, considering their potential adoption in the transition from HFCs to future refrigerants. In the transition towards natural and low GWP refrigerants, fluids like R513A, R516A, R515B and R450A are relevant because they can be used as direct "drop-in" replacements for R134a, without requiring major modifications to existing systems. This study focuses on flow boiling inside channels with azeotropic and quasi-azeotropic mixtures. The effects of mass flux, heat flux, and vapor quality on the heat transfer coefficient of the blends were assessed. To evaluate the feasibility of drop-in substitution of R134a with the tested mixtures, the obtained heat transfer coefficients are compared with those of R134a. Additionally, the new data have been used to propose a modification of the Bertsch et al. [36] correlation to better predict flow boiling heat transfer coefficients. This new version has also been successfully tested against flow boiling data of hydrocarbons, which are expected to be used as refrigerants in heat pumps and refrigeration systems in the near future.

## 2. Experimental approach

### 2.1. Experimental rig and test section

Experiments have been conducted using a circular channel with an internal diameter equal to 0.96 mm. The measuring section and the experimental apparatus are thoroughly described in [3,17]. The

experimental setup (Fig. 1a)) is a closed pumped loop that allows the measurements of the local heat transfer coefficients. The loop is composed by an oil-free inverter-driven gear pump which takes the subcooled liquid refrigerant from the post-condenser and sends it through a Coriolis-effect mass flow meter. By acting on the inverter of the pump and on the throttling valve present in the circuit, the mass flux can be controlled and its stability can be verified from the instantaneous measurements of the Coriolis-effect mass flow meter, by keeping the mass flux variation within 2 %. After the mass flow meter, the refrigerant enters a counter-flow tube-in-tube heat exchanger that works as pre-heater and uses water as secondary fluid. The temperature of the secondary fluid is kept constant by means of a PID control system. The refrigerant exits the pre-heater with a fixed subcooling (usually 2–3 K) and then enters the measuring section, where hot water coming from a thermostatic bath is used to vaporize it. The mass flow rate and temperatures on the water side are measured using a Coriolis-effect mass flow meter and various thermocouples placed along the water circuit. After passing through the test section, the refrigerant enters the condenser to be fully condensed and subcooled. Since the heat is provided by the water, the heat flux is not imposed but depends on the operative conditions. During the experimental campaign, several tests at the same refrigerant mass flux are conducted by varying the water mass flow rate and inlet temperature. By combining the data from several experimental tests, the analysis on the effect of the heat flux and vapor quality is conducted.

The experimental test section is a 0.96 mm internal diameter (ID) tube-in-tube heat exchanger with the refrigerant flowing inside the tube and the secondary hot water flowing in counter-flow on an external annulus. The inner surface roughness *Ra* is equal to 1.3 μm (ISO 4287) and the total length of the measuring sector is equal to 230 mm. The test section used in this work is a horizontally oriented 0.96 mm ID mini-channel and it is presented in Fig. 1b). The tube material is copper and the external water side of the tube has been machined to enhance the heat transfer area and increase the water mixing in correspondence of water thermocouples. In fact, the test section is equipped with fifteen copper-constantan thermocouples inserted in the water path to measure the water temperature profile, while eleven T-type thermocouples are embedded in the wall to measure the wall temperature profile. A relative pressure transducer is used to measure the pressure at the inlet of the measuring section. The outlet pressure is obtained as the difference between the inlet pressure and the measurements of two differential pressure transducers with different measuring ranges.

### 2.2. Composition of the tested mixtures

The tests have been carried out with four different blends. The mixtures were all bought in bottles already prepared by the manufacturers and the charge of the test rig was performed after vacuum was created in the system by a vacuum pump. Finally, to check the composition of the mixture, preliminary tests have been conducted. The agreement between the measured temperature at vapor quality equal to 0.6 and the saturation temperature obtained from Refprop 10 [19] is within 0.2 K (providing as input the measured vapor quality and pressure). The major components of these mixtures, which are all proposed as drop-in substitutes of HFC R134a, are R134a, R1234yf and R1234ze (E). Three of them (R450A, R515B, R513A) are classified as non-flammable and non-toxic (A1) by the ANSI/ASHRAE classification [2], while R516A is classified as mildly flammable (A2L). R450A is a near-

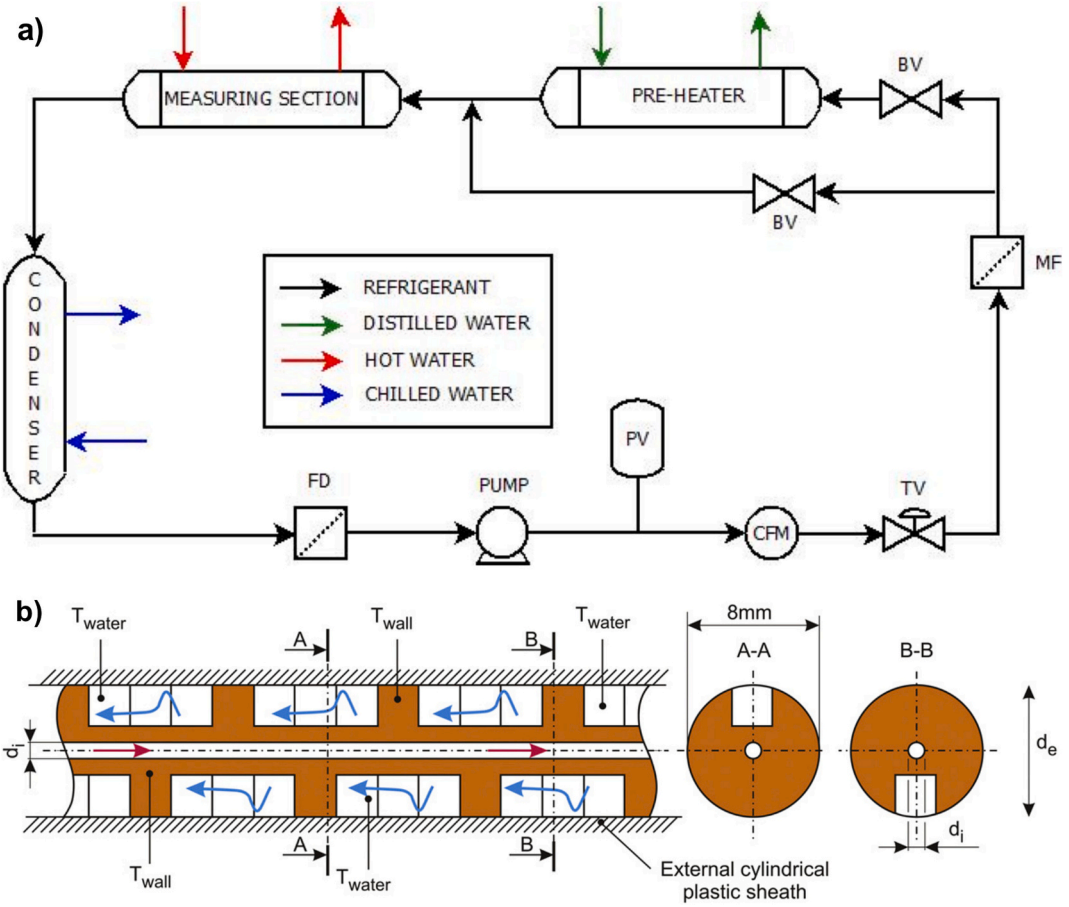


**Fig. 1.** a) Experimental test rig (FD: filter drier; PV: pressure vessel; CFM: Coriolis-effect mass flow meter; TV: throttling valve; MF: mechanical filter; BV: ball valve); b) 0.96 mm ID experimental test section for the measurement of the flow boiling HTC.

azeotropic binary mixture (composed by R1234ze(E)/R134a, 56/44 % by mass, $GWP_{100\text{-years}} = 547$) and it presents a temperature glide $\Delta T_{GL}$ equal to 0.63 K at 30 °C. R515B (composed by R1234ze(E)/R227ea, 91/9 % by mass, $GWP_{100\text{-years}} = 299$) and R513A (composed by R1234yf/R134a, 56/44 % by mass, $GWP_{100\text{-years}} = 629$) are both azeotropic binary blends. Lastly, R516A (composed by R1234yf/R152a/R134a 77.5/14/8.5 % by mass, $GWP_{100\text{-years}} = 131$) is a ternary azeotropic mixture. The $GWP_{100\text{-years}}$ and ODP values are taken from the IPCC Sixth Report (2023) [1]. The thermodynamic properties (obtained from NIST Refprop 10 [19]) of the mixtures tested in this work and their main pure components are reported in Table 1. In the Supplementary Material (Section 2) the temperature composition diagram of the mixture of R1234ze(E) and R134a at 6.77 bar (saturation pressure for R450A) is presented.

### 2.3. Data reduction

As explained above, the heat is provided to the refrigerant flowing in the measuring channel by the water flow, thus the heat flux is not fixed but depends on the operative conditions of the water. For this reason, the local heat flux is determined from the energy balance on the water side (Eq. (1)). The calculations of the heat flux and the HTC, as reported in the following equations, are possible thanks to copper-constantan thermocouples inserted in the water path (15 thermocouples) and on the wall (11 thermocouples), which together with the Coriolis effect mass flow meter are also used to verify the stability of the parameter before the measure is performed:

$$q^{'}(z) = \dot{m}_{wat}\, c_{wat} \left| \frac{\mathrm{d}T_{wat}(z)}{\mathrm{d}z} \right| \tag{1}$$

$$\alpha(z) = \frac{q^{'}(z)}{\pi\, d\, [T_{wall}(z) - T_{sat}(z)]} \tag{2}$$

where $T_{wall}(z)$ is the measured wall temperature, $T_{sat}(z)$ is the local saturation temperature obtained from the refrigerant pressure using Refprop 10 [19] and the local heat flux $q'(z)$ is obtained from the derivative of the polynomial equation interpolating the measured water temperature $\frac{\mathrm{d}T_{wat}(z)}{\mathrm{d}z}$, while $\alpha(z)$ is the local flow boiling HTC at the position $z$. The interpolation procedure does not include the water thermocouples which are in the dry-out region, since these are excluded by the data reduction procedure. As consequence, the maximum value of vapor quality which can be studied in the present work is 0.65. Indeed, higher vapor qualities are in the dry-out region or close to the dry-out region.

The total latent heat gained by the refrigerant from the inlet of the test section to the generic position $q_{lat}(z)$ along the test section can be calculated following Eq. (3). Once this parameter is known, the local vapor quality can be calculated as in Eq. (4):

$$q_{lat}(z) = \dot{m}_{wat}\, c_{wat} \left[ T_{wat}(z) - T_{OUT,wat} \right] - \dot{m}_r \left( h_{sat,L} - h_{IN,r} \right) \tag{3}$$

$$x(z) = \frac{q_{lat}(z)}{\dot{m}_r\, h_{LG}} \tag{4}$$

As can be seen, Eq. (3) gives the mean heat flow rate transferred by the water to vaporize the refrigerant, accounting for the heat required to raise the temperature of the sub-cooled fluid at the entrance of the measuring section to the saturation temperature.

Considering R450A, since it displays a temperature glide equal to 0.63 K at 6.77 bar, the data reduction has been modified compared to the one used for azeotropic mixtures or pure fluids. In particular, the vapor quality and the local refrigerant temperature (that is between the dew and the bubble temperature) are obtained using the local specific enthalpy, pressure and mass composition through the Refprop 10 [19] software. This procedure has been adopted in Berto et al. [20], Azzolin et al. [18,21] and Kondou et al. [22] even with mixtures with larger temperature glide.

### 2.4. Uncertainty analysis

The uncertainty in measured quantities was determined as indicated in the guidelines of the JCGM (2008) [23]. As expressed in the JCGM, the uncertainty of a measured parameter is composed by Type-A and the Type-B contributions. The first comes from repeated observations and is evaluated by statistical methods. In the present work, each experimental point is obtained as the arithmetic mean of 50 signal readings performed in 50 s, and therefore the Type-A uncertainty can be estimated as:

$$u_A = \frac{\sigma_N}{\sqrt{N_P}} \tag{5}$$

where the numerator is the standard deviation of the 50 measures.

The second contribution to the combined uncertainty is the Type-B uncertainty $u_B$ which includes contributions deriving from calibration' procedures and manufacturers' specifications. Type B uncertainties of measured quantities are reported in Table 2.

Once both Type-A and Type-B uncertainty are evaluated, the combined uncertainty $u_C$ can be calculated:

$$u_C = \sqrt{u_A^2 + u_B^2} \tag{6}$$

For a non-directly measured quantities (e.g. HTC, vapor quality, …) that can be expressed as a function $F$ of several measured quantities $X_i$, the combined uncertainty $u_C$ is obtained as combination of the different uncertainties $u_C(X_i)$ related to each measured quantity $X_i$, using the law of propagation of uncertainty:

**Table 1**
Thermodynamic and transport properties of the tested mixtures and their major components at 30 °C saturation temperature. The values were calculated with Refprop 10 [19].

| Fluid | R450A | R515B | R513A | R516A | R1234ze(E) | R1234yf | R134a |
|---|---|---|---|---|---|---|---|
| $GWP_{100\text{-years}}$ | 547 | 299 | 573 | 131 | <1 | <1 | 1300 |
| ASHRAE | A1 | A1 | A1 | A2L | A2L | A2L | A1 |
| ODP | 0 | 0 | 0 | 0 | 0 | 0 | 0 |
| $M$ [kg kmol$^{-1}$] | 108.67 | 117.48 | 108.43 | 102.58 | 114.04 | 114.04 | 102.03 |
| $p_{sat}$ [bar] | 6.77 | 5.75 | 8.21 | 7.98 | 5.78 | 7.84 | 7.7 |
| $p_r$ [/] | 0.18 | 0.16 | 0.23 | 0.22 | 0.16 | 0.23 | 0.19 |
| $\rho_L$ [kg m$^{-3}$] | 1160.6 | 1163.9 | 1141.8 | 1048.9 | 1146.4 | 1073.3 | 1187.5 |
| $\rho_V$ [kg m$^{-3}$] | 34.59 | 31.26 | 43.5 | 39.89 | 30.52 | 46.73 | 37.34 |
| $\mu_L$ [μPa s] | 178.48 | 181.32 | 156.05 | 145.82 | 178.89 | 143.97 | 183.13 |
| $\lambda_L$ [mW m$^{-1}$ K$^{-1}$] | 74.79 | 71.58 | 68.13 | 68.41 | 72.52 | 62.02 | 78.99 |
| $h_{LG}$ [kJ kg$^{-1}$] | 166.34 | 158.24 | 151.88 | 159.46 | 163.06 | 141.24 | 173.10 |
| $\sigma$ [mN m$^{-1}$] | 7.7 | 8.09 | 6.1 | 6.12 | 8.21 | 5.56 | 7.38 |
| $T_{dew}$ [°C] | 30.32 | – | – | – | – | – | – |
| $\Delta T_{GL}$ [K] | 0.63 | – | – | – | – | – | – |

**Table 2**
Type-B experimental uncertainty of measured quantities.

| Measured parameter | Type-B uncertainty |
|---|---|
| Temperature (thermocouples) | ± 0.05 °C |
| Temperature difference (thermopile) | ± 0.03 K |
| Water mass flow rate in sectors 1–2-3 (3.38 mm channel) | ± 0.14 % at 10 kg/h |
| Water mass flow rate in the PS (0.96 mm channel) | ± 0.14 % at 10 kg/h |
| Water mass flow rate in sectors 4–5 (3.38 mm channel) | ± 0.2 % at 10 kg/h |
| Water mass flow rate in the MS (0.96 mm channel) | ± 0.2 % at 10 kg/h |
| Refrigerant mass flow rate | ± 0.2 % at 2 kg/h<br>± 0.1 % at 54 kg/h |
| Absolute pressure | ± 5 kPa<br>(99.7 % confidence level) |
| Pressure difference (>1 kPa) | ± 0.12 kPa<br>(99.7 % confidence level) |
| Pressure difference (<1 kPa) | ± 0.1 kPa<br>(99.7 % confidence level) |
| Test section length and hydraulic diameter | ± 0.02 mm |

$$u_C = \sqrt{\sum_{i=1}^{n} \left[ \left( \frac{\partial F}{\partial X_i} \right)^2 u_C^2(X_i) \right]} \tag{7}$$

where $n$ is the number of measured quantities.

Finally, the expanded uncertainty $U$ is obtained considering a coverage factor $K$ equal to 2 (confidence level equal to 95 %):

$$U = K\, u_C \tag{8}$$

Table 3 reports the expanded standard uncertainty of flow boiling HTC, vapor quality and heat flux. More detailed information for the uncertainty calculation is provided in [17].

## 3. Flow boiling test results

Tests have been run at mean saturation temperature equal to 30 °C and mass flux equal to 300, 400, 500 and 600 kg $m^{-2}$ $s^{-1}$, while the vapor quality varied between 0.04 and 0.65. The obtained flow boiling heat transfer coefficients were studied to evaluate the effect of mass flux, vapor quality and heat flux. The data reduction procedure adopted in the present work excluded all the heat transfer coefficients measured in dry-out conditions. To evaluate if an experimental point was or was not in dry-out, the procedure described by Del Col and Bortolin [24] was implemented. This procedure is based on the evaluation of the standard deviation of the wall temperature measurements: the region of the tube where the dry-out occurs presents the highest standard deviation of the wall temperature. The variation in HTCs within the same mass flux and heat flux range (Figs. 2c)-5c)) is due to the effect of vapor quality, which leads to a reduction in the heat transfer coefficient as it increases.

### 3.1. Effect of mass flux, vapor quality and heat flux

Concerning the effect of mass flux, vapor quality and heat flux, the experimental heat transfer coefficients are plotted in Figs. 2–5. Firstly, the effect of the mass flux is analysed. From Figs. 2c, 3c, 4c and 5c, it can be seen that the experimental data obtained at different mass fluxes for all the refrigerants show a limited or negligible effect of the mass flux on the heat transfer coefficient. The negligible effect of the mass flux on the flow boiling HTC in minichannels was observed also in [5,17,25]. For this reason, in the next graphs, the HTCs of each fluid will be presented without distinction between the mass fluxes.

The heat flux is the parameter that affects the flow boiling heat transfer coefficient the most. This is evident from Figs. 2a, 3a, 4a and 5a, because the increase of the heat flux implies an increment of the heat transfer coefficient when plotted against the vapor quality. In particular, the heat transfer coefficient at 50 kW $m^{-2}$ is on average 63.1 % lower than the flow boiling HTC at 100 kW $m^{-2}$ for R513A. Considering R516A, R515B and R450A, the reduction of the heat flux from 100 kW $m^{-2}$ to 50 W $m^{-2}$ causes a flow boiling heat transfer coefficient reduction of 53.5 %, 48.1 % and 50.9 % respectively. This suggests a predominance of nucleate boiling in the tube for all tested mixtures at the investigated test conditions.

In Figs. 2b, 3b, 4b and 5b the flow boiling heat transfer coefficient have been plotted against the vapor quality at fixed ranges of heat flux ($q = 100 \pm 5$ kW $m^{-2}$, $q = 75 \pm 3$ kW $m^{-2}$ and $q = 50 \pm 2$ kW $m^{-2}$). In this way, it is possible to analyse the effect of the vapor quality. Since the local heat flux is the result of water conditions (temperature and mass flow rate), in order to investigate the effect of vapor quality on the HTC at constant heat flux, data from different experimental runs (performed with the same refrigerant mass flux and saturation temperature) were combined together, filtering the data that fall in a narrow range of heat flux [4]. From the results presented in the figures, it can be observed that the heat transfer coefficient slightly decreases when the vapor quality increases. Considering the mixtures R513A and R516A (mostly composed by R1234yf), the flow boiling heat transfer coefficient decrease due to the vapor quality increment is limited. Indeed, when the vapor quality goes from 0.2 to 0.4 the experimental flow boiling heat transfer coefficient at 100 ± 5 kW $m^{-2}$ reduces on average of 6.5 % for both R513A and R516A, while when considering the experimental point at 50 ± 2 kW $m^{-2}$ the same vapor quality change causes a reduction of the heat transfer coefficient around 3.5 % for both blends. Rather, R515B (mixture richer in R1234ze(E)) showed a higher sensibility to the vapor quality with respect to R513A and R516A. At 100 ± 5 kW $m^{-2}$ and vapor quality going from 0.2 to 0.4 a 9.4 % drop in the heat transfer

**Table 3**
Expanded uncertainty of flow boiling HTC ($U_\alpha$), heat flux ($U_{q'}$) and vapor quality ($U_x$) (coverage factor $k = 2$). The values are referred to the entire database.

| Fluid | $U_\alpha$ [%] | | | $U_{q'}$ [%] | | | $U_x$ [−] | | |
|---|---|---|---|---|---|---|---|---|---|
| | *min* | *mean* | *max* | *min* | *mean* | *max* | *min* | *mean* | *max* |
| R513A | 3.6 | 7.9 | 16.6 | 1.4 | 6.3 | 25.9 | 0.01 | 0.02 | 0.03 |
| R516A | 3.7 | 7.1 | 10.9 | 1.3 | 5.1 | 18.9 | 0.01 | 0.02 | 0.03 |
| R515B | 3.4 | 7.3 | 9.8 | 0.9 | 4.9 | 16.2 | 0.01 | 0.02 | 0.03 |
| R450A | 3.2 | 7.1 | 12.5 | 1.2 | 5.4 | 21.4 | 0.01 | 0.02 | 0.03 |

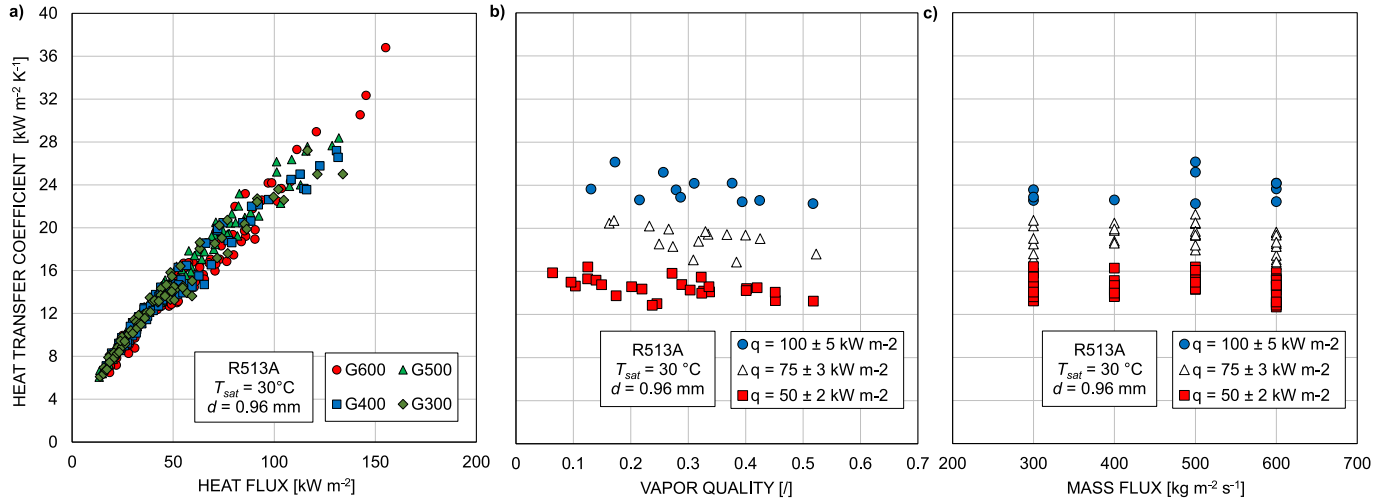


**Fig. 2.** Flow boiling heat transfer coefficients of R513A measured in the 0.96 mm diameter channel at mean saturation temperature of 30 °C: a) HTC versus heat flux; b) HTC versus vapor quality; c) HTC versus mass flux. In b) all the studied mass fluxes have been considered.

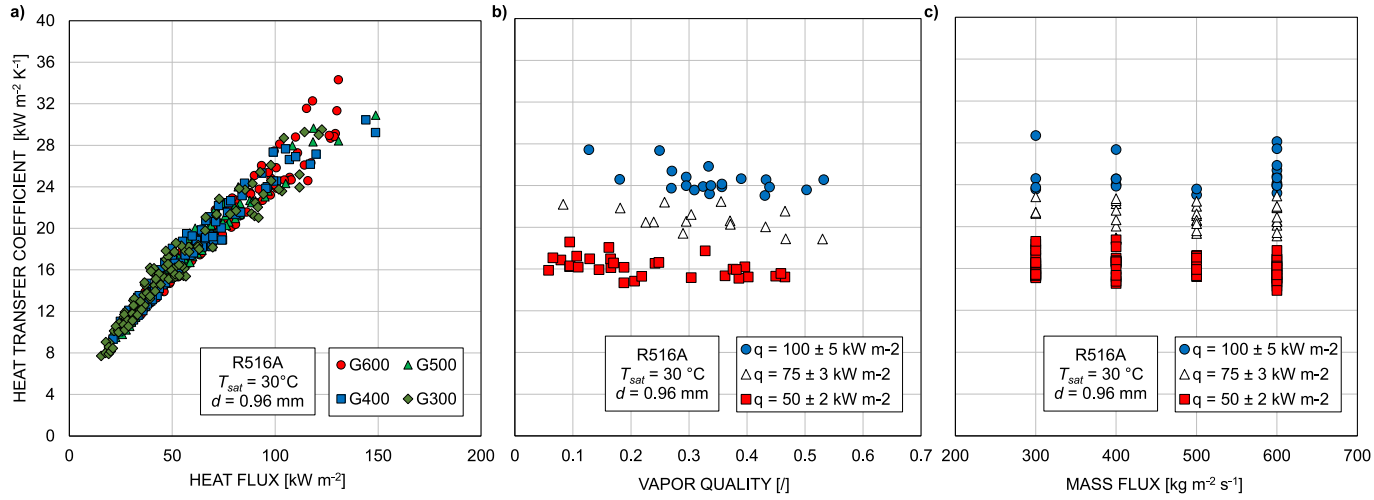


**Fig. 3.** Flow boiling heat transfer coefficients of R516A measured in the 0.96 mm diameter channel at mean saturation temperature of 30 °C: a) HTC versus heat flux; b) HTC versus vapor quality; c) HTC versus mass flux. In b) all the studied mass fluxes have been considered.

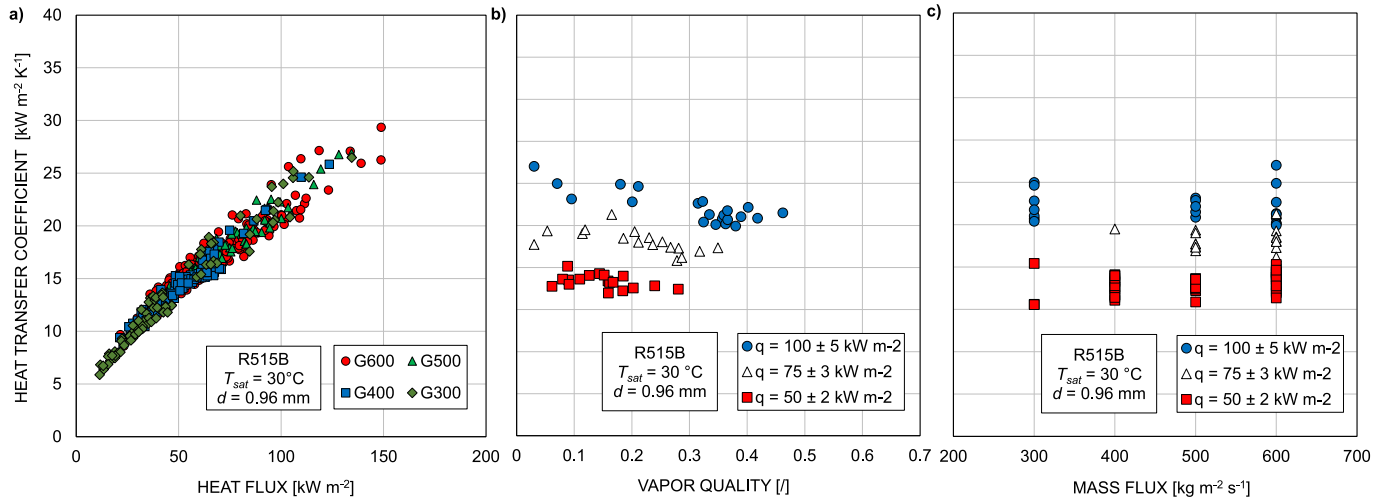


**Fig. 4.** Flow boiling heat transfer coefficients of R515B measured in the 0.96 mm diameter channel at mean saturation temperature of 30 °C: a) HTC versus heat flux; b) HTC versus vapor quality; c) HTC versus mass flux. In b) all the studied mass fluxes have been considered.

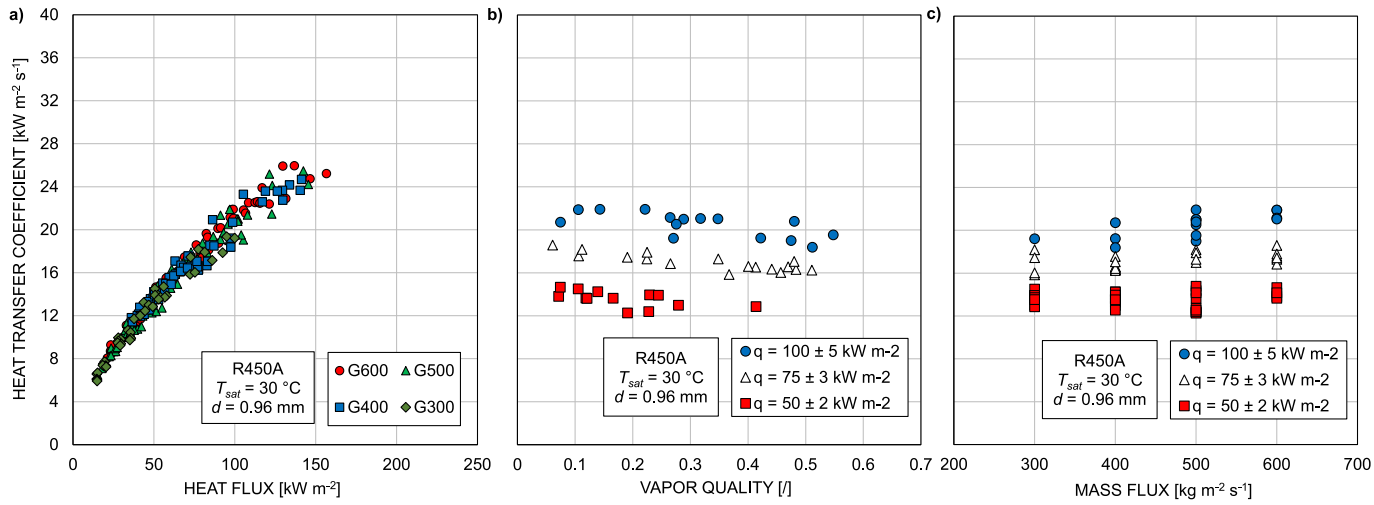


**Fig. 5.** Flow boiling heat transfer coefficients of R450A measured in the 0.96 mm diameter channel at mean saturation temperature of 30 °C: a) HTC versus heat flux; b) HTC versus vapor quality; c) HTC versus mass flux. In b) all the studied mass fluxes have been considered.

coefficient can be observed. While at 50 ± 2 kW $m^{-2}$, when the vapor quality goes from 0.2 to 0.3 the heat transfer coefficient presents a 4 % drop. Thus, at both 100 ± 5 kW $m^{-2}$ and 50 ± 2 kW $m^{-2}$, R515B displays a higher reduction of the HTC than R513A and R516A. Lastly, R450A for vapor quality increasing from 0.2 to 0.4 at both 100 ± 5 kW $m^{-2}$ and 50 ± 2 kW $m^{-2}$ displays a flow boiling HTC reduction around 5.6 %.

For the examined mixtures, and the present experimental conditions, it can be summarized that an increase in heat flux significantly enhances the heat transfer coefficient, while the vapor quality increase slightly reduces the heat transfer coefficient, and mass flux contribution on the flow boiling heat transfer is negligible. These trends for the flow boiling HTC in minichannels were observed in previous papers [4,18]. These works analysed the flow boiling of pure fluids and azeotropic mixtures. Moreover, the same behaviour for flow boiling in minichannels was reported by Shiferaw et al. [26], Anwar et al. [27] and Bertsch et al. [28], showing that the heat transfer coefficient increases with the heat flux and slightly decreases with the vapor quality, while no effect of the mass flux was observed.

The present experimental data can be interpreted as evidence that the dominant heat transfer mechanism is nucleate boiling. In fact, for all the fluids, we observed a strong dependence of the heat transfer coefficient on the heat flux, no dependence on the mass flux and a slight decrease of the heat transfer coefficient with vapor quality. This behaviour is consistent with a heat transfer condition controlled by nucleate boiling, where boiling occurs at nucleation sites on the tube wall surface. With higher heat flux, more nucleation sites become activated, resulting in a higher heat transfer coefficient; conversely, an increase in vapor quality reduces the presence of liquid, leading to fewer active nucleation sites.

It is true that the three-zone evaporation model by Thome et al. [29], based on the assumption of convective heat transfer in the confined bubble regime without contribution from nucleate boiling (with the exception for the bubble formation frequency) predicts an increasing trend of the HTC with the heat flux and a decreasing trend of the HTC with the vapor quality, as found in the present experiments. However, as reported in Shiferaw et al. [26], the three-zone model predicts also an effect of the mass flow rate on the HTC, effect that is not found in the present experimental data. Furthermore, recent visualizations performed in even smaller channels (0.4 mm), in which the bubble confinement effect is expected to be even more evident, show the presence of bubbles nucleation. In particular, Tibiriçá and Ribatski [30] investigated flow boiling with R134a and R245fa inside a 0.4 mm microchannel and they detected vapor bubbles departing from the channel wall and nucleation sites active for all the flow patterns. This strengthens the assumption of nucleate boiling as dominant heat transfer mechanism in the experimental conditions investigated in the present paper.

The nucleate boiling heat transfer coefficient can be calculated considering the correlation from Cooper [31]:

$$HTC = 55\, p_r^{0.12-0.2\,\log Rp}\,(-\log p_r)^{-0.55}\, M^{-0.5}\, q'^{0.67} \tag{9}$$

where $Rp$ is the wall surface roughness according to DIN 4762/1, $M$ is the molecular mass of the considered fluid, $q'$ is the heat flux and $p_r$ is the reduced pressure (the ratio between the actual pressure and the critical pressure of the fluid). In Eq. (9) the heat transfer coefficient is a function of the heat flux power to 0.67.

As reported in the work of Bortolin et al. [32], the nucleate boiling phenomenon can be active also in annular flow regime inside small diameter channels since numerous bubbles were detected by the authors at the tube wall. The hypothesis that nucleate boiling is the dominant mechanism can be supported by an analysis of the experimental heat transfer coefficient data as a function of heat flux in the 0.96 mm channel as presented in Fig. 6. Data from selected vapor quality ranges were analysed, particularly within $x = 0.3 \pm 0.05$ (Figs. 6a-b) and $x = 0.2 \pm 0.05$ (Figs. 6c-d). The choice to present two distinct vapor quality ranges for all four mixtures was made to confirm the findings under varying conditions. As observed in Figs. 6a and 6b for $x = 0.3 \pm 0.05$, all the mixtures exhibit a relation with heat flux that aligns with the Cooper equation. Specifically, the exponent of the power function interpolation is equal to 0.64, 0.68, 0.65 and 0.66 respectively for R516A, R513A, R515B and R450A. The same behaviour can also be seen for the other vapor quality range $x = 0.2 \pm 0.05$ (Figs. 6c-d), with all the mixtures showing a power law coherent with the Cooper correlation. This is of particular interest especially for R450A, which despite presenting a not-null temperature glide, even if lower than 1 K, did not show a significant deviation from the prediction of the Cooper equation.

### 3.2. Comparison between mixtures and their pure components

The comparison between the four tested mixtures and the major pure fluids components R134a, R1234yf and R1234ze(E) is presented in Fig. 7. The data of the pure fluids were taken in the same experimental apparatus at similar operative conditions and can be found in [4,17,25]. The comparison reported in Fig. 7 in terms of heat transfer coefficient versus heat flux has been made considering a vapor quality $x = 0.3 \pm 0.05$. The heat transfer coefficients of the mixtures and of the pure fluids

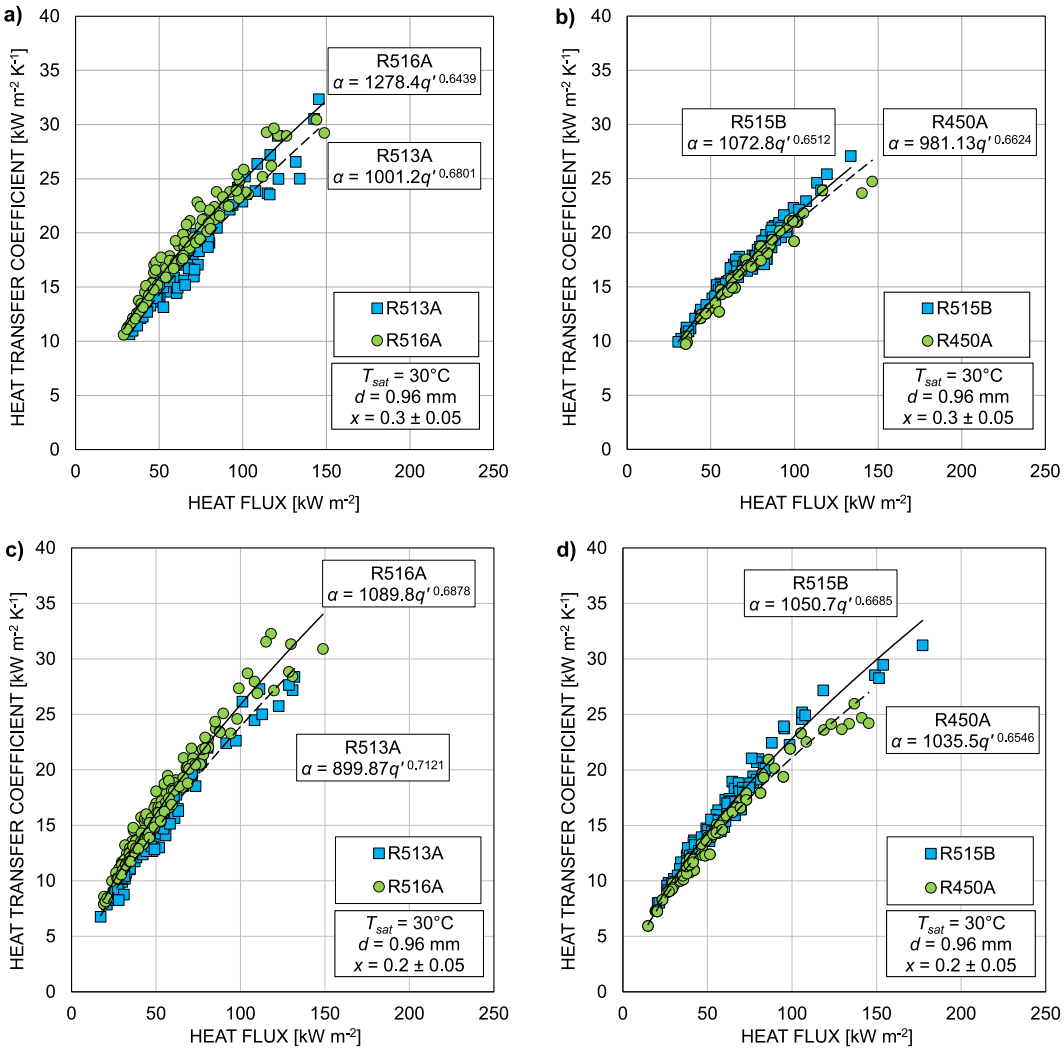


**Fig. 6.** Flow boiling heat transfer coefficients of the tested mixtures measured in the 0.96 mm diameter channel at mean saturation temperature of 30 °C for a-b) $x = 0.3 \pm 0.05$ and c-d) $x = 0.2 \pm 0.05$. The placement of the fluids in the graphs is based on the pure HFO component.

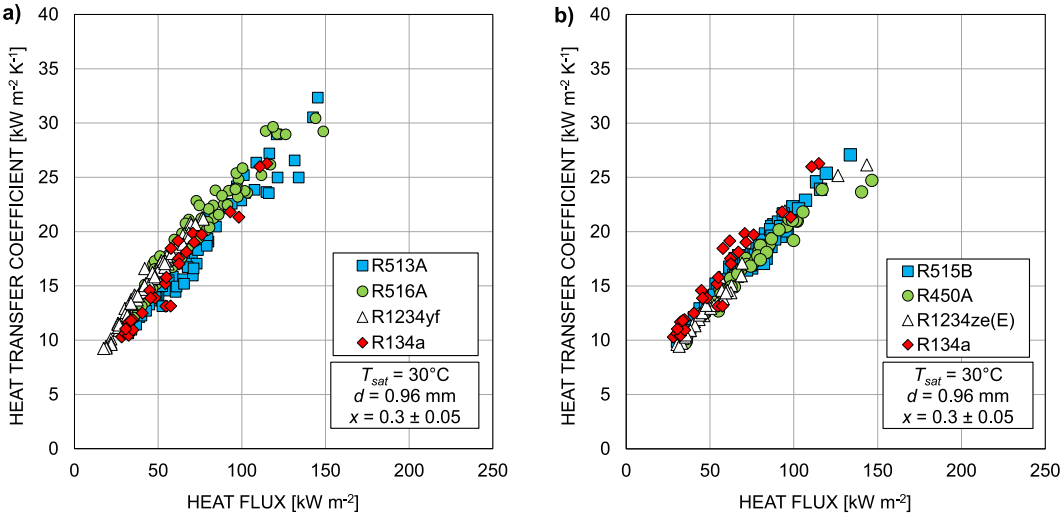


**Fig. 7.** Comparison of flow boiling heat transfer coefficients of a) R513A and R516A and b) R515B and R450A with the flow boiling heat transfer coefficients of the major components. The reported HTCs are measured in the 0.96 mm diameter channel at a mean saturation temperature of 30 °C and $x = 0.3 \pm 0.05$. The placement of the fluids in the graphs is based on the pure HFO component.

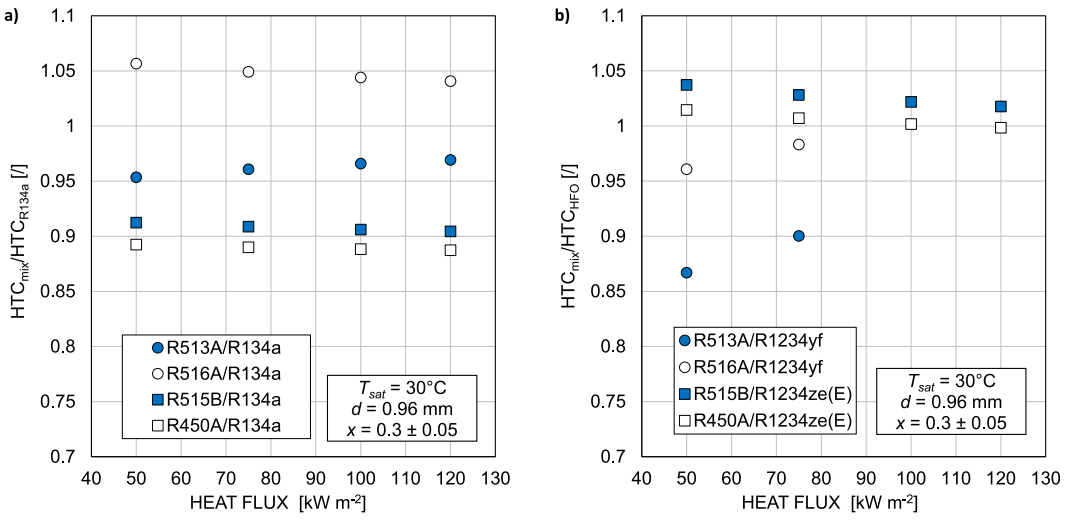


**Fig. 8.** Comparison among the flow boiling HTCs of the tested mixtures and the pure components. The comparison was performed considering all mass fluxes and vapor quality $x = 0.3 \pm 0.05$. The comparison with R1234yf at 100 kW m$^{-2}$ and 120 kW m$^{-2}$ was not possible since there are no experimental points for it at these heat fluxes.

present a similar trend. In particular, from Fig. 7a): when comparing the heat transfer coefficient of R513A with those of R516A, it emerged that R516A presents HTC on average 8 % higher than R513A; when comparing the HTCs of R513A and R516A with those of R134a (Fig. 8a) the maximum difference is 5 %, thus within the experimental uncertainty range. Moreover, when comparing the HTCs of R513A and R516A with those of R1234yf (Fig. 8b), R516A heat transfer coefficient differs from those of R1234yf by less than 5 % while R513A present an average reduction with respect to R1234yf around 10 %. This difference between the flow boiling HTCs of R1234yf and R513A can be explained with a combination of the different properties of the two fluids in particular molecular mass, reduced pressure and surface tension.

Differently from R513A and R516A it can be observed from Fig. 7b) and Fig. 8a) that R515B and R450A present lower heat transfer coefficients with respect to R134a: the reduction is respectively equal to 10 % and 15 % for R515B and R450A. The reduction can be explained by the lower value of molecular mass and the higher value of reduced pressure of R134a that, following Eq. (9), are key parameters of nucleate boiling. When compared to R1234ze(E), both R450A and R515B present comparable heat transfer coefficients with a difference below 4 % for both fluids (see Fig. 8b). The same behaviour can be observed when comparing R515B and R450A. The heat transfer coefficient of R515B is slightly higher than that of R450A, however, the differences are never higher than 6 %. Since the molecular mass and the reduced pressure are similar for these fluids, the smaller difference of R450A can be a consequence of its near azeotropic behaviour.

Summarizing, most of the differences in terms of heat transfer coefficients between the tested mixtures and the main pure components (R134a, R1234ze(E) and R1234yf) are within the experimental uncertainty. The only exception is the comparison of the heat transfer coefficients between R134a and R515B, as well as between R450A and R134a, where a difference greater than 10 % was observed.

In Fig. 9, the flow boiling heat transfer coefficients of R450A and R513A were compared with the heat transfer coefficients of the pure components R134a and the hydrofluoroolefins R1234yf and R1234ze (E). The comparison was carried out at vapor quality equal to 0.3 and heat flux equal to 70 kW m$^{-2}$ (as shown in Section 3.1, in this condition there is no effect of the mass flux on the HTC). As can be seen, the heat transfer coefficient of both mixtures is lower than the one resulting from a linear interpolation of the heat transfer coefficients measured with the pure fluids (9.1 % for R450A and 4.7 % for R513A). The deviation of R513A is within the uncertainty of the experimental tests, thus confirming its azeotropic behaviour, while the difference is slightly higher than the average error for R450A. This can be explained by the near-azeotropic behaviour of the mixture.

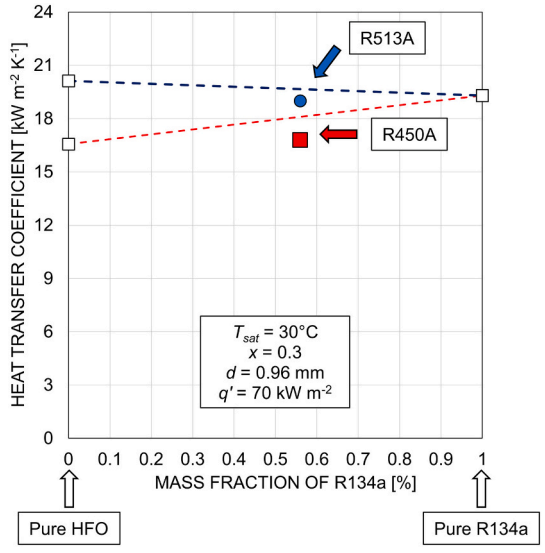


**Fig. 9.** Experimental heat transfer coefficients of R450A, R513A and the pure components R1234yf, R1234ze(E) and R134a measured in the 0.96 mm channel at vapor quality equal to 0.3 and heat flux equal to 70 kW m$^{-2}$. Dashed lines refer to the ideal linear behaviour. Mass composition equal to 0 corresponds to pure R1234yf or R1234ze(E) and equal to 1 corresponds to pure R134a.

## 4. Comparison with vaporization models

### 4.1. Models for pure fluids and azeotropic mixtures

The heat transfer coefficients measured during flow boiling of the four blends were used to assess the predictions of five different HTC models. These are semi-empirical correlations that can be found in the literature. In particular, the models of Sun and Mishima [33], Lazarek and Black [34], Gungor and Winterton [35], Bertsch et al. [36] and Thome et al. [29,37] were used. These models have been selected since they were developed using a large experimental database, encompassing

different fluids (natural refrigerants, HFCs, HCFCs, HFOs, …) and a wide range of operative conditions (mass fluxes between 20 and 3000 kg $m^{-2}$ $s^{-1}$, diameters between 0.16 mm and 6 mm, vapor qualities between 0.01 and 0.99, saturation pressures between 1 bar and 57 bar). In previous works conducted in minichannels [4,18,26], these models were used to predict heat transfer data coming from different experimental databases. From these papers, similar accuracy of the predictions of the models with respect to the experimental data was obtained, especially with the model of Sun and Mishima [33] and Bertsch et al. [36]. Among the previous correlations, the Sun and Mishima [33] and the Lazarek and Black [34] models consider the nucleate boiling phenomenon as the dominant one. On the contrary, the models of Gungor and Winterton [35] and Bertsch et al. [36] are based on the Chen [38] approach, in which both the contribution of the nucleate boiling and convective evaporation components are considered:

$$\alpha = S\,\alpha_{nb} + E\,\alpha_{cb} \tag{10}$$

In Eq. (10), the nucleate boiling HTC is multiplied by the suppression factor $S$ while the convective boiling HTC is multiplied by the enhancement factor $E$.

Differently from the previous correlations, the model of Thome et al. [29,37] evaluates the heat transfer coefficient following a description of the physical phenomenon based on a frequency analysis of the bubble and considering the film evaporation as the dominant factor.

The Gungor and Winterton [35] model and the Bertsch et al. [36] model, adopt the Cooper correlation to evaluate the nucleate boiling. In his original work, Cooper [31,39] stated that the equation as reported in Eq. (9) should be used when investigating pool boiling over plane surfaces while in the case of pool boiling around copper tubes, Eq. (9) should be multiplied by an additional constant equal to 1.7. In the present analysis, the models were evaluated with both versions of the Cooper correlation. This was done to identify the best version of the Cooper correlation for each fluid. In fact, the models that require the Cooper correlation recommend to use Eq. (9) or they don't specify which version to use. However, in previous experimental campaigns with HFOs and HFCs performed by the present authors, the version of Cooper equation for pool boiling over circular copper tube was found to give better predictions [4,17]. In Table 4 the results of the comparison are reported. As can be seen in Table 4, the model by Bertsch et al. [36] presents a better agreement with the experimental data when Cooper correlation (Eq. (9)) is multiplied by 1.7. Indeed, the average absolute deviation with all fluids is less than 20 %. On the contrary, the model of Gungor and Winterton [35] gives a better agreement with the experimental results when Eq. (9) is used (Cooper correlation for pool boiling over plane surfaces), with an average absolute deviation equal to 22.7 %. This difference can be explained by considering the other equations adopted in the two correlations: the two models are both based on the Chen correlation, but their suppression and enhancement factors are not the same, resulting in a different prediction. In particular, for the investigated mixtures, the Bertsch et al. [36] model shows larger deviation from the experimental data when using the basic version of the Cooper equation, as it does not adequately account for the effect of the nucleate boiling component even at low vapor quality values, when the suppression factor is close to zero. Consequently, increasing the nucleate boiling HTC led to more accurate predictions.

Thus, in the following comparison, the model of Gungor and Winterton [35] has been considered using Eq. (9) for the nucleate boiling heat transfer coefficient, while in the model of Bertsch et al. [36] Eq. (9) was multiplied by 1.7.

Figs. 10 and 11 show the comparison with the models of Sun and Mishima [33] and Bertsch et al. [36]. The results of the comparison are presented as the ratio of the calculated HTC to the experimental HTC. This value is presented as function of the vapor quality (Fig. 10) and as function of the heat flux (Fig. 11). These two models were chosen since they have been developed for channels with a diameter range that covers the present minichannel. The mean percentage error $e_R$, the mean absolute percentage error $e_{AB}$ and the standard deviation $\sigma_N$ of the five models for all the fluids are reported in Table 5.

In Figs. 10–11, it can be seen that both models tend to underestimate the flow boiling heat transfer coefficient for R513A and R516A. Nevertheless, some differences can be observed between their predictions. Indeed, the model of Bertsch et al. [36] foresees an important effect of the vapor quality on the HTC which in this case is not seen experimentally. For the present data, the heat transfer coefficient is slightly affected by $x$ (see Figs. 2–5). The absolute deviation of the model increases from 5 to 10 % to more than 40 % for both R513A and R516A when the vapor quality is increased from 0.1 to 0.55. This is a consequence of the high penalization that the correlation applies to the nucleate boiling part at high vapor quality. On the contrary, the correlation by Sun and Mishima [33] does not appear to be subjected to an effect of the vapor quality. In particular, the mean absolute error of Sun and Mishima [33] model for R513A is equal to 19.7 % and for R516A is equal to 24.7 % and for both fluids this value is constant with the vapor quality. For Bertsch et al. [36] correlation the mean absolute errors are equal to 9 % for R513A and to 11.8 % for R516A. Lastly, considering the effect of the heat flux on the correlations of Sun and Mishima [33] and Bertsch et al. [36] similar conclusions can be drawn. In fact, both models' prediction did not show a particular trend as function of the heat flux.

Considering the predictions of the models with R515B and R450A, reported in Figs. 10–11, the results are similar to those obtained with the other blends. The model of Sun and Mishima [33] underestimates the heat transfer coefficient with a mean absolute error equal to 27.5 % and 18.9 % considering R515B and R450A respectively. The mean absolute error of the model of Bertsch et al. [36] increases with the vapor quality and the increases are comparable to those of R513A and R516A. The mean absolute error of the model is equal to 14.6 % and to 8 % for R515B and R450A respectively.

Looking at the values reported in Table 5, it emerges that the model of Bertsch et al. [36] is the more accurate among the models based on

**Table 4**
Mean percentage error $e_R$, mean absolute percentage error $e_{AB}$ and standard deviation $\sigma_N$ of the model of Gungor and Winterton [35] and Bertsch et al. [36] with the two versions of the Cooper [31,39] correlation. The value reported for R450A are corrected for the near-azeotropic behaviour as reported in Section 4.2.

| | Gungor and Winterton [35] | | | Bertsch et al. [36] | | |
|---|---|---|---|---|---|---|
| | $e_R$ [%] | $e_{AB}$[%] | $\sigma_N$ [%] | $e_R$ [%] | $e_{AB}$[%] | $\sigma_N$ [%] |
| Cooper [31,39] correlation for nucleate boiling over plane surfaces (Eq. (9)) | | | | | | |
| R513A | 31.9 % | 31.9 % | 15.7 % | −39.6 % | 39.6 % | 5.6 % |
| R516A | 16.6 % | 17.1 % | 11.8 % | −45.6 % | 45.6 % | 5.1 % |
| R515B | 21.7 % | 21.7 % | 8.2 % | −46.1 % | 46.1 % | 3.5 % |
| R450A | 20.2 % | 20.2 % | 9.7 % | −45.2 % | 45.2 % | 4.5 % |
| Cooper [31,39] correlation for nucleate boiling over round copper tubes (Eq. (9)*1.7) | | | | | | |
| R513A | 76.0 % | 76.0 % | 27.7 % | −10.1 % | 11.4 % | 10.6 % |
| R516A | 53.4 % | 53.4 % | 21.9 % | −19.2 % | 19.2 % | 8.3 % |
| R515B | 59.6 % | 59.6 % | 15.5 % | −21.4 % | 21.4 % | 5.9 % |
| R450A | 53.7 % | 53.7 % | 17.7 % | −19.8 % | 19.8 % | 7.5 % |

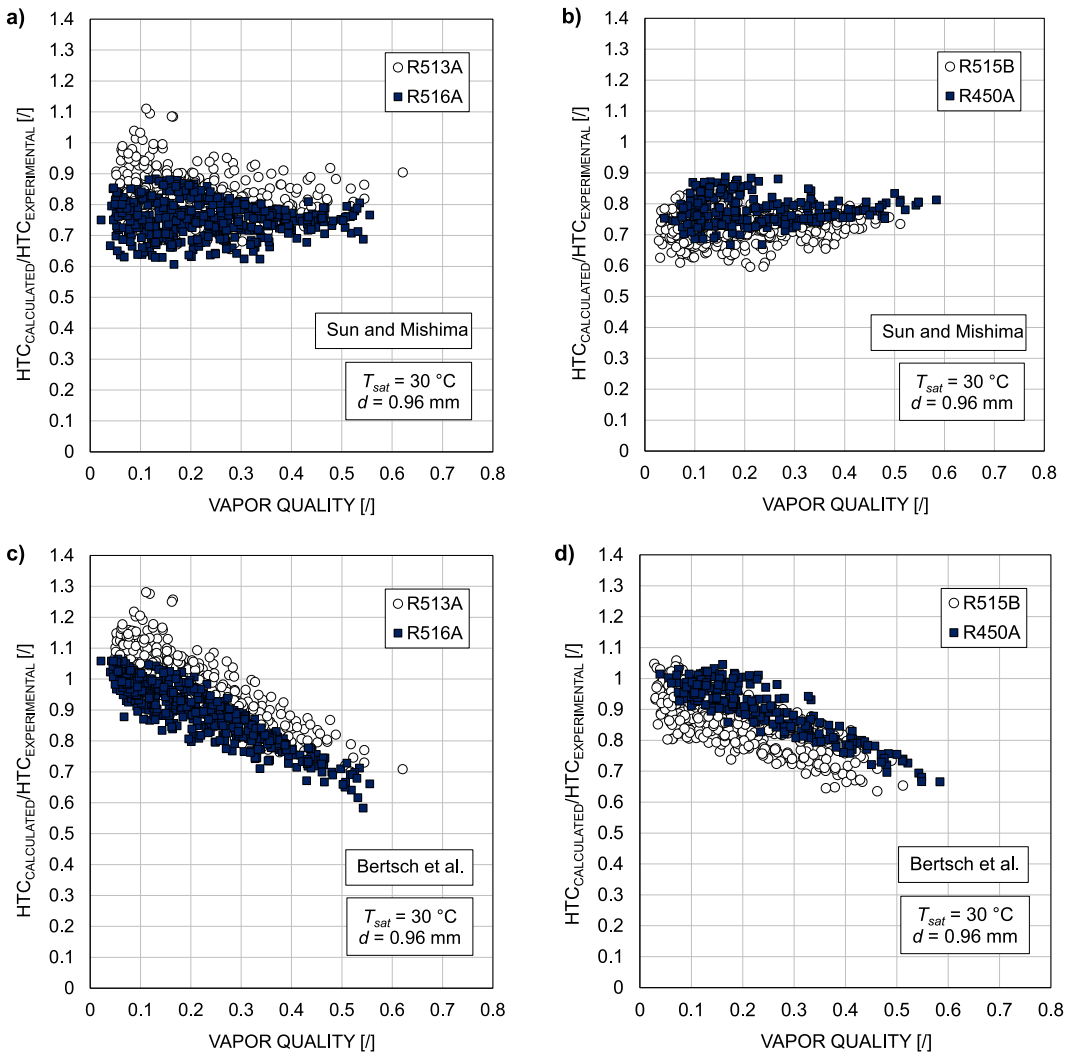


**Fig. 10.** Comparison of the flow boiling heat transfer coefficients of the tested mixtures with the models of a-b) Sun and Mishima [33] and c-d) Bertsch et al. [36]. The comparison is made as function of the vapor quality. The placement of the fluids in the graphs is based on the pure HFO component.

the Chen [38] correlation, while the model of Sun and Mishima [33] is the more accurate for the nucleate boiling type correlations. The model by Gungor and Winterton [35] shows a mean absolute error around 25 %, while for the model of Bertsch et al. [36] the average $e_{AB}$ is equal to 17 %. The predictions from the models of Lazarek and Black [34] and Sun and Mishima [33] are less accurate compared to Bertsch et al. [36] correlation, displaying $e_{AB}$ equal to 28 % and 23 %, respectively. Regarding the model of Thome et al. [29,37], the average $e_{AB}$ is generally the highest compared to the other models ($e_{AB}$ = 34 %).

Considering the two correlations with the highest accuracy (Sun and Mishima [33] and Bertsch et al. [36]), the best one is a Chen-type correlation (Bertsch et al. [36]). This seemed in contradiction with the conclusion of the vaporization process being mostly dominated by nucleate boiling. However the model by Sun and Mishima [33] does not foresee an effect of the vapor quality on the heat transfer coefficient. Moreover, the prediction of the model of Bertsch et al. [36] is less accurate at higher vapor quality because the flow boiling component of the model is not able to compensate the excessive reduction of the nucleate boiling, which is still the dominant mechanism. This can be caused by the equation chosen by the authors for the suppression factor of the nucleate boiling. Since in the case of the present minichannel there is an effect of the vapor quality even though not high as the one foreseen by the model of Bertsch et al. [36], both models could be improved.

### 4.2. Correlations for zeotropic mixtures

The models used in this work have been developed for pure fluids and azeotropic mixtures. The tested blends are azeotropic except for R450A, which is a near-azeotropic mixture with a temperature glide equal to 0.63 K at 30 °C saturation temperature. For this reason, following the work of Azzolin et al. [18] a correction can be necessary to consider the non-azeotropic behaviour of the blend, although the temperature glide is below 1 K. The correction terms presented in Azzolin et al. are here adopted because they proved to be effective in the prediction of the flow boiling HTC of zeotropic mixtures in previous studies by the present authors. In the work of Azzolin et al., a two-step correction is proposed. The first is the application of correction factor $F_c$ by Thome [40]:

$$F_c = \left[1 + \left(\frac{\alpha_f \, \Delta T_{GL}}{\dot{q}}\right)\left(1 - e^{-\frac{B\,\dot{q}}{\rho_L \, \Delta h_m \, \beta_L}}\right)\right]^{-1} \tag{11}$$

This correction factor is multiplied by the boiling number Bo for nucleate boiling correlations [33,34], or for the nucleate boiling HTC contribution in Chen type correlations [35,36]. In Eq. 11, $B$ is a scaling factor considered equal to 1, $\Delta h_m$ is the isobaric enthalpy change at the given composition of the mixture, and the liquid mass transfer coefficient $\beta_L$ is assumed equal to 0.0003 m s$^{-1}$. Lastly, the ideal flow boiling

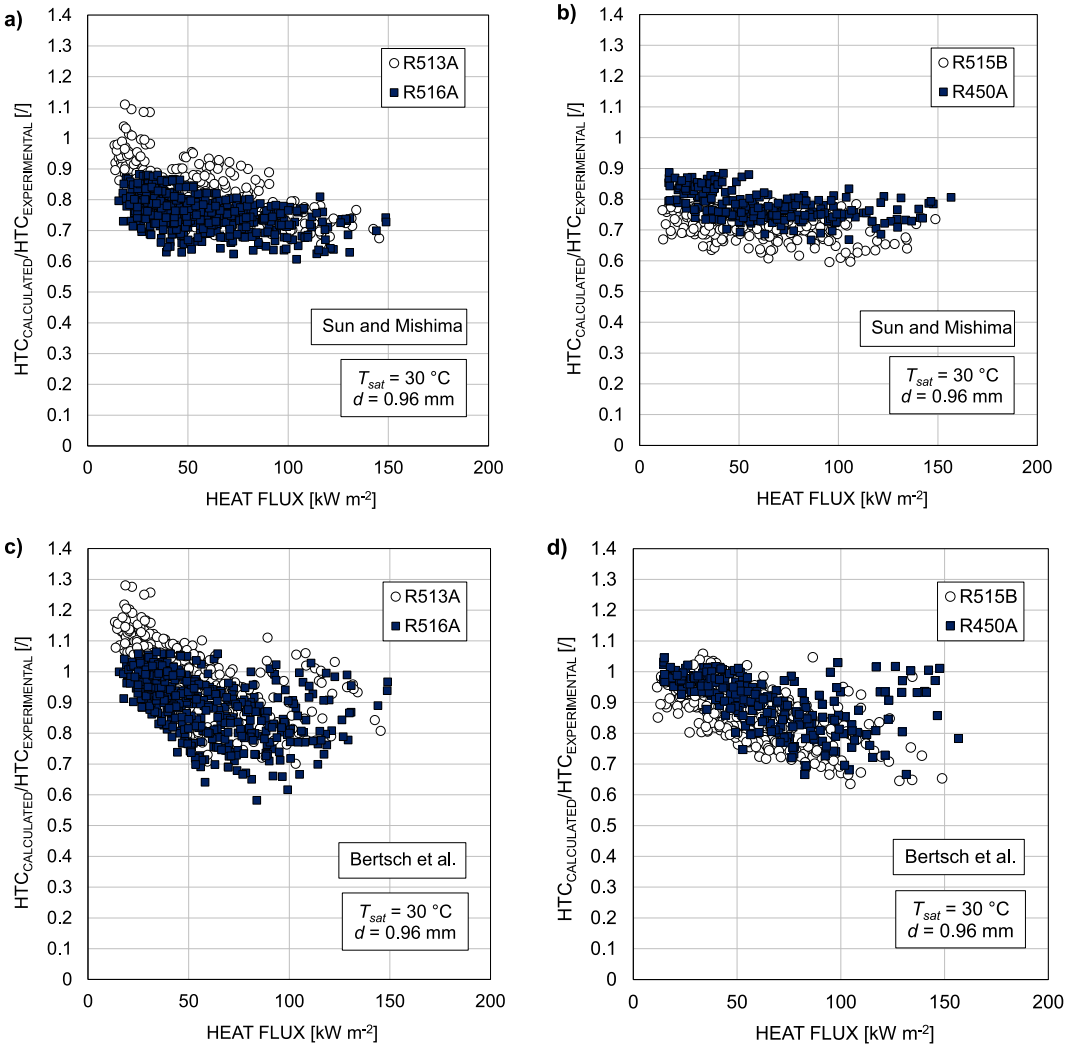


**Fig. 11.** Comparison of the flow boiling heat transfer coefficients of the tested mixtures with the models of a-b) Sun and Mishima [33] and c-d) Bertsch et al. [36]. The comparison is made as function of the heat flux. The placement of the fluids in the graphs is based on the pure HFO component.

heat transfer coefficient $\alpha_f$ is calculated with a correlation for pure fluids.

The second correction is introduced to consider the penalization of the HTC due to the additional thermal resistance and the sensible heating at the liquid-vapor interface (Cavallini et al. [41]). This correction was first developed by Bell and Ghaly [42]:

$$\alpha_m = \left( \frac{1}{\alpha_f} + \frac{x\, c_G\, \Delta T_{GL}/\Delta h_m}{\alpha_G} \right)^{-1} \tag{12}$$

where $\alpha_G$ is the vapor phase convective HTC, $c_G$ is the vapor phase specific heat and $\alpha_f$ is the flow boiling heat transfer coefficient. Thus, the Bell and Ghaly [42] correction is applied after the nucleate boiling correction factor. These two correction factors are computed as described above for all the considered models, with the only exception of the Thome et al. [29,37] model where only the correction of Bell and Ghaly [42] was applied. The calculated values considering the additional mass transfer coefficients for R450A are reported in Table 5, while Fig. 12 presents the results of the comparison with the models of Sun and Mishima [33] and Bertsch et al. [36]. Since the temperature glide of R450A is below 1 K at 6.77 bar the introduction of the corrections causes only a slight change in the heat transfer coefficient predicted by the models, as can be seen from the graphs and also from the values reported in Table 5. From the observation of Fig. 9, the experimental heat transfer coefficient of R450A is 9.1 % lower if compared with a linear interpolation of the HTCs of the pure components and this is due to the nearly azeotropic behaviour of the mixture. The error $e_{AB}$ changes from 18.9 % to 24 % for the Sun and Mishima [33] model, from 23.6 % to 29.2 % for the Lazarek and Black [34] model, from 33.5 % to 20.2 % for the Gungor and Winterton [35] model, from 11.3 % to 19.8 % for the Bertsch et al. [36] model and from 26.5 % to 28.2 % for the Thome et al. [29,37] model. Generally, the corrections did not improve the models' prediction accuracy: since the models for pure fluids already underestimated the heat transfer coefficient, the introduction of a mass transport resistance results in an even higher reduction of the predicted HTC.

### *4.3. Proposed modified suppression factor to be included in the model of Bertsch et al. [36]*

An analysis of Figs. 10 and 11 reveals that the predictive accuracy of the Bertsch et al. [36] declines as vapor quality increases. Specifically, the model exhibits optimal performance at low vapor quality, but its precision progressively diminishes with rising vapor quality. In particular, the Bertsch et al. [36] model is highly sensitive to increases in vapor quality, whereas the experimental data did not show such a significant reduction. This led to the hypothesis that the suppression factor for nucleate boiling requires further investigation. In fact, the suppression factor is a linear function of the vapor quality (as reported in Eq.

**Table 5**
Mean percentage error $e_R$, mean absolute percentage error $e_{AB}$ and standard deviation $\sigma_N$ of the models of Sun and Mishima [33], Lazarek and Black [34], Gungor and Winterton [35], Bertsch et al. [36] and Thome et al. [29,37] for the tested fluids. (*) Results for R450A are obtained using the correlations for zeotropic mixtures.

| Fluid | $G$ [kg m$^{-2}$ s$^{-1}$] | Sun and Mishima [33] | | | Lazarek and Black [34] | | | Gungor and Winterton [35] | | | Bertsch et al. [36] | | | Thome et al. [31,29,37] | | |
|---|---|---|---|---|---|---|---|---|---|---|---|---|---|---|---|---|
| | | $e_R$ [%] | $e_{AB}$[%] | $\sigma_N$ [%] | $e_R$ [%] | $e_{AB}$[%] | $\sigma_N$ [%] | $e_R$ [%] | $e_{AB}$[%] | $\sigma_N$ [%] | $e_R$ [%] | $e_{AB}$[%] | $\sigma_N$ [%] | $e_R$ [%] | $e_{AB}$[%] | $\sigma_N$ [%] |
| R513A | 300 | −20.5 % | 20.5 % | 6.5 % | −29.5 % | 29.5 % | 4.8 % | 30.1 % | 30.1 % | 13.9 % | −13.2 % | 13.9 % | 10.4 % | −31.2 % | 31.2 % | 4.8 % |
| | 400 | −18.4 % | 18.4 % | 5.3 % | −26.0 % | 26.0 % | 4.6 % | 31.9 % | 31.9 % | 11.8 % | −10.2 % | 10.6 % | 7.1 % | −31.1 % | 31.1 % | 4.3 % |
| | 500 | −18.2 % | 18.2 % | 7.1 % | −25.4 % | 25.4 % | 3.5 % | 29.5 % | 29.5 % | 15.9 % | −10.7 % | 11.5 % | 10.1 % | −32.1 % | 32.1 % | 7.1 % |
| | 600 | −13.4 % | 14.3 % | 9.4 % | −19.2 % | 19.2 % | 5.7 % | 36.2 % | 36.3 % | 18.9 % | −6.2 % | 9.4 % | 10.1 % | −29.7 % | 29.7 % | 8.2 % |
| | mean | −17.6 % | 17.9 % | 7.1 % | −25.0 % | 25.0 % | 4.6 % | 31.9 % | 31.9 % | 15.7 % | −10.1 % | 11.4 % | 10.6 % | −31.0 % | 31.0 % | 6.1 % |
| R516A | 300 | −27.8 % | 27.8 % | 5.6 % | −34.9 % | 34.9 % | 5.2 % | 13.5 % | 13.9 % | 10.9 % | −22.2 % | 22.2 % | 8.4 % | −41.4 % | 41.4 % | 4.4 % |
| | 400 | −25.9 % | 25.9 % | 4.6 % | −31.3 % | 31.3 % | 4.4 % | 17.1 % | 17.6 % | 11.1 % | −21.5 % | 21.5 % | 9.1 % | −42.3 % | 42.3 % | 4.9 % |
| | 500 | −23.0 % | 23.0 % | 4.9 % | −28.7 % | 28.7 % | 4.0 % | 18.7 % | 18.9 % | 11.9 % | −17.5 % | 17.5 % | 8.3 % | −40.9 % | 40.9 % | 5.4 % |
| | 600 | −22.0 % | 22.0 % | 5.3 % | −25.3 % | 25.3 % | 4.1 % | 18.1 % | 18.7 % | 12.9 % | −15.4 % | 15.4 % | 7.6 % | −40.4 % | 40.4 % | 5.6 % |
| | mean | −24.7 % | 24.7 % | 5.1 % | −30.0 % | 30.0 % | 4.4 % | 16.6 % | 17.1 % | 11.8 % | −19.2 % | 19.2 % | 8.3 % | −41.3 % | 41.3 % | 5.1 % |
| R515B | 300 | −29.0 % | 29.0 % | 5.4 % | −36.6 % | 36.6 % | 5.5 % | 21.4 % | 21.4 % | 10.4 % | −21.5 % | 21.5 % | 5.5 % | −40.6 % | 40.6 % | 3.2 % |
| | 400 | −27.0 % | 27.0 % | 3.3 % | −32.4 % | 32.4 % | 4.3 % | 24.2 % | 24.2 % | 5.5 % | −21.2 % | 21.2 % | 5.6 % | −41.6 % | 41.6 % | 4.3 % |
| | 500 | −27.6 % | 27.6 % | 3.0 % | −29.6 % | 29.6 % | 4.2 % | 20.1 % | 20.1 % | 6.9 % | −21.8 % | 21.8 % | 6.5 % | −42.7 % | 42.7 % | 5.4 % |
| | 600 | −26.2 % | 26.2 % | 4.4 % | −27.1 % | 27.1 % | 6.0 % | 20.9 % | 20.9 % | 8.5 % | −21.1 % | 21.1 % | 5.9 % | −43.4 % | 43.4 % | 5.3 % |
| | mean | −27.5 % | 27.5 % | 4.0 % | −31.4 % | 31.4 % | 5.0 % | 21.2 % | 21.2 % | 8.2 % | −21.4 % | 21.4 % | 5.9 % | −42.1 % | 42.1 % | 4.6 % |
| R450A | 300 | −19.4 % | 19.4 % | 4.7 % | −29.7 % | 29.7 % | 5.6 % | 38.6 % | 38.6 % | 9.9 % | −10.5 % | 10.5 % | 7.4 % | −24.8 % | 24.8 % | 4.1 % |
| | 400 | −21.1 % | 21.1 % | 3.4 % | −22.7 % | 22.7 % | 6.9 % | 29.6 % | 29.6 % | 6.5 % | −13.6 % | 14.1 % | 9.8 % | −26.8 % | 26.8 % | 7.4 % |
| | 500 | −17.5 % | 17.5 % | 5.1 % | −22.1 % | 22.1 % | 7.2 % | 35.1 % | 35.1 % | 12.9 % | −9.8 % | 10.1 % | 8.8 % | −26.6 % | 26.6 % | 6.3 % |
| | 600 | −17.8 % | 17.8 % | 4.1 % | −19.9 % | 19.9 % | 6.5 % | 32.2 % | 32.2 % | 11.7 % | −10.5 % | 10.5 % | 8.2 % | −27.9 % | 27.9 % | 6.3 % |
| | mean | −18.9 % | 18.9 % | 4.3 % | −23.6 % | 23.6 % | 6.6 % | 33.5 % | 33.5 % | 10.9 % | −11.1 % | 11.3 % | 8.6 % | −26.5 % | 26.5 % | 6.0 % |
| R450A (*) | 300 | −24.2 % | 24.2 % | 5.1 % | −34.3 % | 34.3 % | 4.2 % | 23.9 % | 23.9 % | 9.7 % | −18.7 % | 18.7 % | 7.1 % | −26.7 % | 26.7 % | 4.0 % |
| | 400 | −26.5 % | 26.5 % | 3.1 % | −28.9 % | 28.9 % | 5.5 % | 16.3 % | 16.3 % | 5.5 % | −22.6 % | 22.6 % | 7.8 % | −28.9 % | 28.9 % | 6.9 % |
| | 500 | −22.6 % | 22.6 % | 5.2 % | −27.7 % | 27.7 % | 5.7 % | 21.8 % | 21.8 % | 11.2 % | −18.5 % | 18.5 % | 7.9 % | −28.1 % | 28.1 % | 6.2 % |
| | 600 | −22.9 % | 22.9 % | 4.4 % | −25.9 % | 25.9 % | 4.9 % | 19.7 % | 19.7 % | 9.9 % | −19.4 % | 19.4 % | 7.3 % | −29.3 % | 29.3 % | 6.4 % |
| | mean | −24.0 % | 24.0 % | 4.4 % | −29.2 % | 29.2 % | 5.1 % | 20.2 % | 20.2 % | 9.7 % | −19.8 % | 19.8 % | 7.5 % | −28.2 % | 28.2 % | 5.9 % |

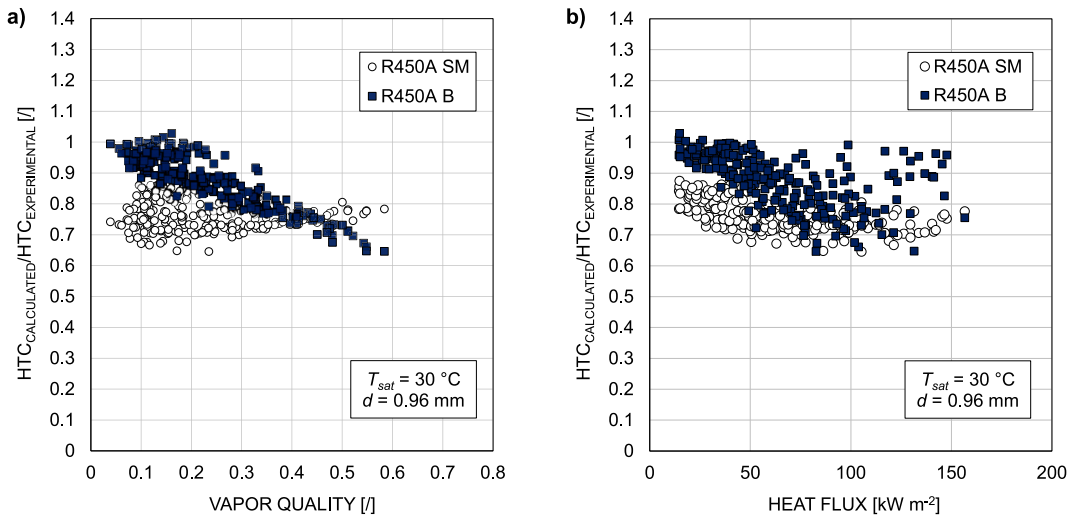


**Fig. 12.** Comparison of the flow boiling heat transfer coefficients of R450A with the models of Sun and Mishima [33] (SM) and Bertsch et al. [36] (B) corrected with the Thome [40] and Bell and Ghaly [42] corrections. The comparison is made as function of the a) vapor quality and b) heat flux.

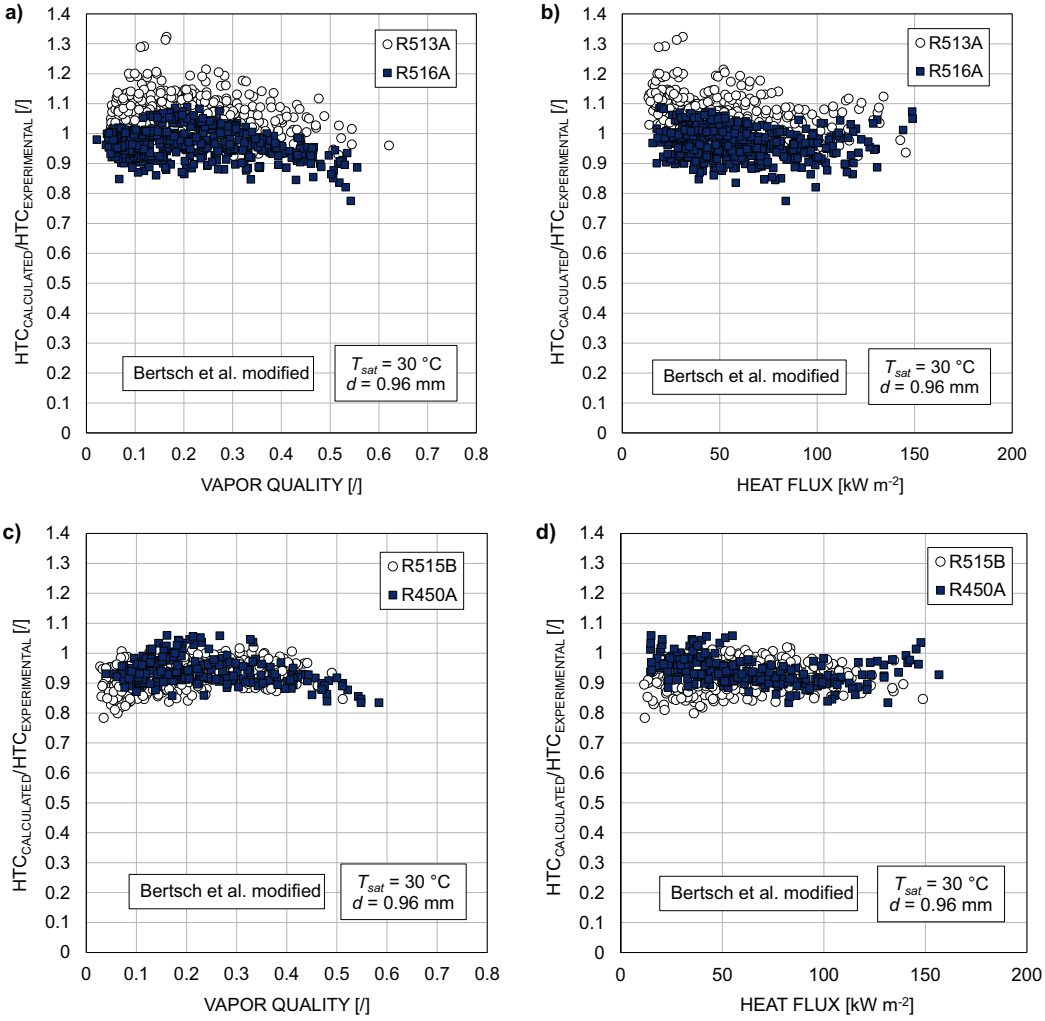


**Fig. 13.** Prediction of the model of Bertsch et al. [36] with the suppression factor for the nucleate boiling modified as in Eq. (12) for all fluid studied. The correction for the near-azeotropic behaviour of R450A have been considered.

**Table 6**
Thermodynamic and transport properties of R32, R1234yf, propane and propylene at 30 °C saturation temperature. The values were calculated with Refprop 10 [19].

| Fluid | R290 | R1270 | R1234yf | R32 |
|---|---|---|---|---|
| $GWP_{100\text{-years}}$ | 3 | 2 | <1 | 675 |
| $M$ [kg kmol$^{-1}$] | 44.09 | 42.08 | 114.04 | 52 |
| $p_{sat}$ [bar] | 10.79 | 13.05 | 7.84 | 19.27 |
| $p_{red}$ [/] | 0.25 | 0.29 | 0.23 | 0.33 |
| $\rho_L$ [kg m$^{-3}$] | 484.4 | 497.5 | 1073.3 | 939.62 |
| $\rho_V$ [kg m$^{-3}$] | 23.45 | 27.72 | 46.73 | 54.78 |
| $\mu_L$ [μPa s] | 92.13 | 90.01 | 143.97 | 107.23 |
| $\lambda_L$ [mW m$^{-1}$ K$^{-1}$] | 91.41 | 103.13 | 62.02 | 122.10 |
| $h_{LG}$ [kJ kg$^{-1}$] | 326.7 | 324.98 | 141.24 | 260.4 |
| $\sigma$ [mN m$^{-1}$] | 6.43 | 6.34 | 5.56 | 6.00 |

(13)) and this progressively reduces the nucleate boiling component. The result is that the difference between experimental and calculated heat transfer coefficients is higher when increasing the vapor quality. To address this issue, in the present work, a modification of the original Bertsch et al. [36] model is proposed (the complete original model is reported in the Supplementary material). In the model of Bertsch et al. [36], the suppression factor is calculated as:

$$S = 1 - x \tag{13}$$

The authors of the model stated that, among the various functions that could be chosen, this was the simplest one that could give the required trend for the nucleate boiling heat transfer when the vapor quality increases. In the present case, the nucleate boiling phenomena is highly contributing to the heat transfer process and thus the suppression factor $S$ has an important impact on the prediction accuracy of the model strongly decreasing the heat transfer coefficient with the increasing vapor quality (see Fig. 10). The following equation for the suppression factor is proposed to modify the penalization on the nucleate boiling component while keeping a simple equation as originally stated in Bertsch et al. [36].

$$S = 1 - x^2 \tag{14}$$

When considering this new version of the suppression factor, the predicted value of the heat transfer coefficient calculated with the model of Bertsch et al. [36] are shown in Fig. 13. For R450A the values reported have been corrected as shown previously. As can be seen, in the new version of the correlation the prediction accuracy as a function of the vapor quality is improved. The average absolute deviation is below 8 % with all the tested fluids, in particular, is equal to 5.6 %, 4.9 %, 4.1 % and 6.6 % with R513A, R516A, R515B and R450A respectively.

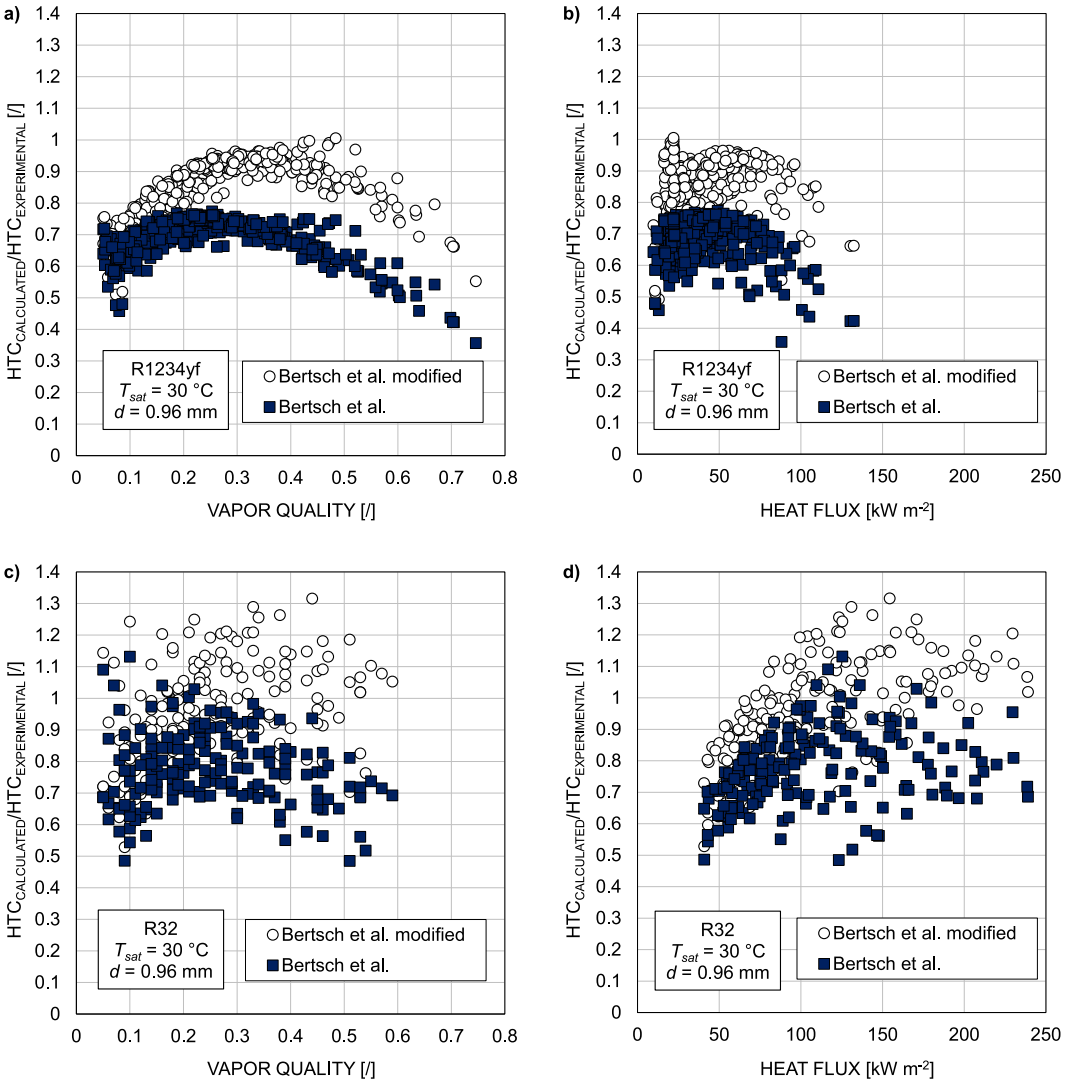


**Fig. 14.** Prediction of the model of Bertsch et al. [36] and the proposed modification to the model of Bertsch et al. (modified suppression factor for the nucleate boiling as in Eq. (6)) for R1234yf and R32. Data of these fluid taken from [4,25].

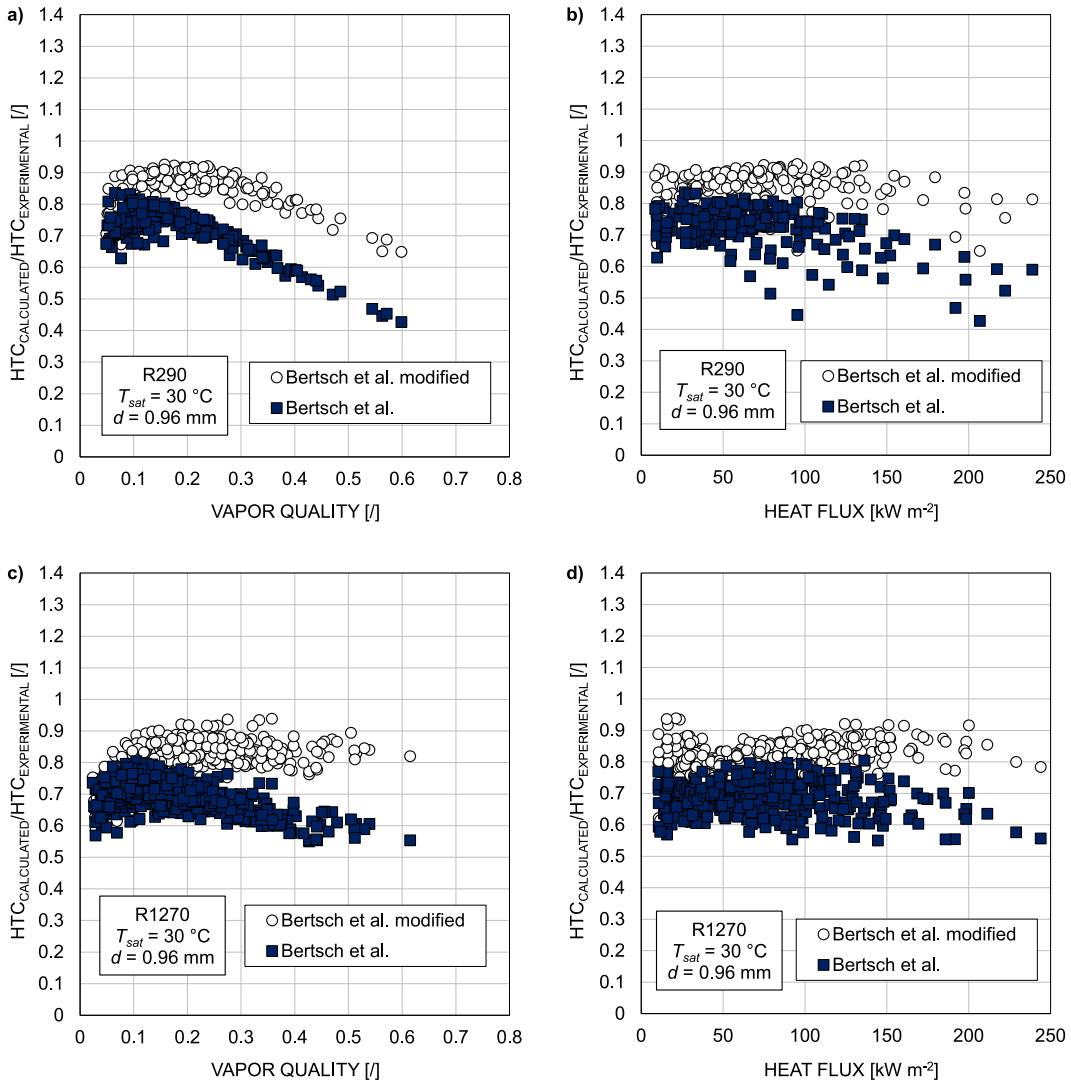


**Fig. 15.** Prediction of the model of Bertsch et al. [36] and the proposed modification to the model of Bertsch et al. (modified suppression factor for the nucleate boiling as in Eq. (6)) for propane and propylene. Data of these fluid taken from [43,44].

The modified Bertsch et al. [36] correlation proposed in this work has been compared with other fluids, in particular HFC R32, HFO R1234yf and hydrocarbons propane (R290) and propylene (R1270). The data for these fluids were taken from Del Col et al. [4,25,43,44]. These fluids were chosen because their thermodynamic and transport properties are different (Table 6) compared to the new database of the mixtures.

In Fig. 14 the corrected model for R1234yf and R32 was compared to the model of Bertsch et al. [36] without modification. For these fluids, the model was applied with the Cooper equation for pool boiling over copper tubes (Eq. (9) multiplied by 1.7), the same as the previously tested mixture. As can be seen from Fig. 14, the proposed modification leads to a general improvement in the prediction of the model. In particular, the mean absolute deviation with R1234yf drops from 32.4 % with the model of Bertsch et al. [36] to 15.6 % with the modification proposed in the present work. Furthermore, the prediction accuracy reduction with the increasing vapor quality is less important with the new model. Fig. 15 shows the comparison between the original Bertsch et al. [36] correlation and the modified correlation presented in this paper for propane and propylene. In this case, the Cooper correlation was applied as reported in Eq. (9) and thus without the factor 1.7. In fact, for these fluids, the model prediction is more accurate with this version of the Cooper correlation. The reason behind this can be found in the development of the correlation of Cooper [39]: the database used in the work of Cooper was interpolated to find the constant that fit the data. Since the database was wide and included a lot of fluids (with molecular mass from 2 kg kmol$^{-1}$ to 200 kg kmol$^{-1}$), the constant obtained from the interpolation procedure may fit the data for natural refrigerant, whereas not working properly for the synthetic refrigerant. The modified correlation is able to increase the accuracy of the model for both the hydrocarbons: with propane the average deviation with the modified model is equal to 20.2 % while with the original model is equal to 31.6 %. Similarly with propylene, the adoption of the new suppression factor results in an absolute deviation equal to 15.4 % compared to 27.4 %, as before. Moreover, it can be easily seen from Figs. 14–15 that the modification of the model presented in this work led to the better result and the decrease of the prediction accuracy when the vapor quality increases is reduced when adopting the new proposed correlation. For instance, at vapor quality equal to 0.4, the model of Bertsch et al. [36] displayed a deviation always higher than 30 % with R1234yf, R32, propane and propylene, while the proposed correlation reduced this deviation to a maximum value of 20 %.

To summarize, the procedure suggested in this paper to modify the Bertsch et al. [36] correlation is as follows: 1) for synthetic fluids and mixtures the authors suggest the use of the modified suppression factor as reported in Eq. (14) for the nucleate boiling and the Cooper equation

for pool boiling over circular copper tubes (Eq. (9) multiplied by 1.7); 2) for hydrocarbons the authors suggest the use of the modified suppression factor as reported in Eq. (14) for the nucleate boiling and the Cooper equation for pool boiling over plane surfaces as reported in Eq. (9).

## 5. Conclusions

In this paper the flow boiling heat transfer of four mixtures of HFC/HFO was studied. The effects of mass velocity, heat flux and vapor quality on the heat transfer coefficient of R513A (R1234yf/R134a, 56/44 % by mass), R516A (R1234yf/R152a/R134a 77.5/14/8.5 % by mass), R515B (R1234ze(E)/R227ea, 91/9 % by mass) and R450A (R1234ze(E)/R134a, 56/44 % by mass) were analysed. The tests were conducted inside a 0.96 mm internal diameter horizontal smooth tube, using hot water to promote the boiling.

The results of the experimental study can be briefly listed as follows.

- The heat flux has the greater impact on the flow boiling heat transfer. The heat transfer coefficient increment is always on average higher than 45 % for all blends when the heat flux is doubled from 50 kW $m^{-2}$ to 100 kW $m^{-2}$.
- The mass flux does not affect the flow boiling heat transfer coefficient, while the vapor quality poorly affect the heat transfer phenomenon, causing HTC reductions never higher than 6.5 % except for R515B for which the vapor quality increase from 0.2 to 0.4 causes a reduction up to 9.5 %.
- The heat transfer coefficient as function of the heat flux followed the correlation for nucleate boiling by Cooper [31], thereby supporting the assumption that nucleate boiling is the dominant mechanism.
- R513A and R516A display flow boiling heat transfer coefficients comparable with those of R134a, with a maximum difference of 5.5 %, indicating a similar behaviour of these mixtures in the dry expansion evaporators.
- Regarding the prediction of the flow boiling heat transfer coefficient, the model of Bertsch et al. [36] showed the lowest mean absolute percentage error and mean percentage error for all the tested fluids, with maximun values $e_{AB} = 14.1$ % and $e_R = -14.6$ % with R515B. The prediction by the model of Sun and Mishima [33] is slightly less accurate, but the model presents a lower standard deviation (5.1 % on average with all the fluids).
- The proposed modification of the Bertsch et al. [36] correlation was found to give a better agreement with respect to the original model with all the four mixtures tested. Moreover, the modified model was tested with R32, R1234yf, propane and propylene and resulted in a mean absolute error always lower or equal to 20 %.

## CRediT authorship contribution statement

**Nicolò Mattiuzzo:** Writing – original draft, Visualization, Validation, Software, Methodology, Investigation, Formal analysis, Data curation, Conceptualization. **Marco Azzolin:** Writing – original draft, Supervision, Resources, Project administration, Methodology, Investigation, Funding acquisition, Data curation, Conceptualization. **Arianna Berto:** Writing – review & editing, Data curation. **Stefano Bortolin:** Writing – review & editing, Methodology. **Davide Del Col:** Writing – review & editing, Supervision, Project administration, Methodology, Conceptualization.

## Declaration of competing interest

The authors declare the following financial interests/personal relationships which may be considered as potential competing interests:

Marco Azzolin reports financial support was provided by European Commission. If there are other authors, they declare that they have no known competing financial interests or personal relationships that could have appeared to influence the work reported in this paper.

## Acknowledgements

Financial support by the European Commission - Next Generation EU, Missione 4, Componente 1, CUP C53D23001690006, “Environmentally friendly high-glide refrigerant blends for high-temperature heat pumps and next-generation refrigerators”, project code: 20229J4EMW is acknowledged.

This work has been also supported by MASE – ENEA program “Ricerca di Sistema Elettrico – Piano Triennale di Realizzazione PTR 2022–2024 – Tecnologie per la penetrazione efficiente del vettore elettrico negli usi finali”.

## Appendix A. Supplementary data

Supplementary data to this article can be found online at https://doi.org/10.1016/j.icheatmasstransfer.2025.108929.

## Data availability

Data will be made available on request.

## References

[1] Intergovernamental Panel on Climate Change IPCC, Climate Change 2023: Synthesis Report, UNEP - UN Environment Programme, 2023, pp. 35–115, https://doi.org/10.59327/IPCC/AR6-9789291691647.
[2] American Society of Heating Refrigeration and Air-Conditioning Engineers, ASHRAE Standard 34: Designation and Safety Classification of Refrigerants, 2016, 2016.
[3] D. Del Col, M. Bortolato, M. Azzolin, S. Bortolin, Condensation heat transfer and two-phase frictional pressure drop in a single minichannel with R1234ze(E) and other refrigerants, Int. J. Refrig. 50 (2015) 87–103, https://doi.org/10.1016/j.ijrefrig.2014.10.022.
[4] D. Del Col, S. Bortolin, D. Torresin, A. Cavallini, Flow boiling of R1234yf in a 1 mm diameter channel, Int. J. Refrig. 36 (2012) 353–362, https://doi.org/10.1016/j.ijrefrig.2012.10.026.
[5] A. Diani, S. Mancin, L. Rossetto, Flow boiling heat transfer of R1234yf inside a 3.4mm ID microfin tube, Exp. Thermal Fluid Sci. 66 (2015) 127–136, https://doi.org/10.1016/j.expthermflusci.2015.03.019.
[6] A. Diani, S. Mancin, L. Rossetto, R1234ze(E) flow boiling inside a 3.4 mm ID microfin tube, Int. J. Refrig. 47 (2014) 105–119, https://doi.org/10.1016/j.ijrefrig.2014.07.018.
[7] Z. Li, K. Liang, H. Jiang, Experimental study of R1234yf as a drop-in replacement for R134a in an oil-free refrigeration system, Appl. Therm. Eng. 153 (2019) 646–654, https://doi.org/10.1016/j.applthermaleng.2019.03.050.
[8] J. Sieres, I. Ortega, F. Cerdeira, E. Álvarez, Drop-in performance of the low-GWP alternative refrigerants R452B and R454B in an R410A liquid-to-water heat pump, Appl. Therm. Eng. 182 (2021), https://doi.org/10.1016/j.applthermaleng.2020.116049.
[9] A. Mota-Babiloni, J. Haro-Ortuño, J. Navarro-Esbrí, Á. Barragán-Cervera, Experimental drop-in replacement of R404A for warm countries using the low GWP mixtures R454C and R455A, Int. J. Refrig. 91 (2018) 136–145, https://doi.org/10.1016/j.ijrefrig.2018.05.018.
[10] L. Molinaroli, A. Lucchini, L. Pietro, M. Colombo, Drop-in analysis of R450A and R513A as low-GWP alternatives to R134a in a water-to-water heat pump, Int. J. Refrig. 135 (2022) 139–147, https://doi.org/10.1016/j.ijrefrig.2021.12.007.
[11] H.G. Ramírez-Hernández, A. Morales-Fuentes, F.A. Sánchez-Cruz, S. Méndez-Díaz, H.D. García-Lara, S. Martínez-Martínez, Experimental study on the operating characteristics of a display refrigerator phasing out R134a to R1234ze(E) and its binary blends, Int. J. Refrig. 138 (2022), https://doi.org/10.1016/j.ijrefrig.2022.03.004.
[12] C. Mateu-Royo, A. Mota-Babiloni, J. Navarro-Esbrí, Á. Barragán-Cervera, Comparative analysis of HFO-1234ze(E) and R-515B as low GWP alternatives to HFC-134a in moderately high temperature heat pumps, Int. J. Refrig. 124 (2021) 197–206, https://doi.org/10.1016/j.ijrefrig.2020.12.023.
[13] P. Makhnatch, A. Mota-Babiloni, A. López-Belchí, R. Khodabandeh, R450A and R513A as lower GWP mixtures for high ambient temperature countries: experimental comparison with R134a, Energy 166 (2019) 223–235, https://doi.org/10.1016/j.energy.2018.09.001.
[14] A.K.S. Al-Sayyab, J. Navarro-Esbrí, A. Barragán-Cervera, S. Kim, A. Mota-Babiloni, Comprehensive experimental evaluation of R1234yf-based low GWP working fluids for refrigeration and heat pumps, Energy Convers. Manag. 258 (2022), https://doi.org/10.1016/j.enconman.2022.115378.
[15] A. Diani, L. Rossetto, 513A flow boiling heat transfer inside horizontal smooth tube and microfin tube, Int. J. Refrig. 107 (2019) 301–314, https://doi.org/10.1016/j.ijrefrig.2019.07.023.

[16] M.A. Kedzierski, D. Kang, Horizontal convective boiling of R1234yf, R134a, and R450A within a micro-fin tube, Int. J. Refrig. 88 (2018) 538–551, https://doi.org/10.1016/j.ijrefrig.2018.02.021.
[17] S. Bortolin, M. Bortolato, M. Azzolin, D. Del Col, Comparative experimental procedures for measuring the local heat transfer coefficient during flow boiling in a microchannel, Exp. Thermal Fluid Sci. 90 (2018) 231–245, https://doi.org/10.1016/j.expthermflusci.2017.09.017.
[18] M. Azzolin, S. Bortolin, D. Del Col, Predicting methods for flow boiling heat transfer of a non-Azeotropic mixture inside a single microchannel, Heat Transf. Eng. 37 (2016) 1136–1147, https://doi.org/10.1080/01457632.2015.1111114.
[19] E.W. Lemmon, I.H. Bell, M.L. Huber, M.O. McLinden, NIST Standard Reference Database 23: Reference Fluid Thermodynamic and Transport Properties-REFPROP, Version 10.0, National Institute of Standards and Technology, 2018, https://doi.org/10.18434/T4/1502528.
[20] A. Berto, M. Azzolin, S. Bortolin, C. Guzzardi, D. Del Col, Measurements and modelling of R455A and R452B flow boiling heat transfer inside channels, Int. J. Refrig. 120 (2020) 271–284, https://doi.org/10.1016/j.ijrefrig.2020.08.007.
[21] M. Azzolin, S. Bortolin, D. Del Col, Flow boiling heat transfer of a zeotropic binary mixture of new refrigerants inside a single microchannel, Int. J. Therm. Sci. 110 (2016) 83–95, https://doi.org/10.1016/j.ijthermalsci.2016.06.026.
[22] C. Kondou, D. Baba, F. Mishima, S. Koyama, Flow boiling of non-azeotropic mixture R32/R1234ze(E) in horizontal microfin tubes, Int. J. Refrig. 36 (2013) 2366–2378, https://doi.org/10.1016/j.ijrefrig.2013.07.009.
[23] Group 1 of the Joint Committee for Guides in Metrology (JCGM/WG1), Evaluation of Measurement Data — Guide to the Expression of Uncertainty in Measurement, Int. Organ. Stand. Geneva ISBN 50, 2008, p. 134.
[24] D. Del Col, S. Bortolin, Investigation of dryout during flow boiling in a single microchannel under non-uniform axial heat flux, Int. J. Therm. Sci. 57 (2012) 25–36, https://doi.org/10.1016/j.ijthermalsci.2012.01.020.
[25] D. Del Col, S. Bortolin, L. Rossetto, Convective boiling inside a single circular microchannel, Int. J. Heat Mass Transf. 67 (2013) 1231–1245, https://doi.org/10.1016/j.ijheatmasstransfer.2013.08.050.
[26] D. Shiferaw, T.G. Karayiannis, D.B.R. Kenning, Flow boiling in a 1.1 mm tube with R134a: experimental results and comparison with model, Int. J. Therm. Sci. 48 (2009) 331–341, https://doi.org/10.1016/j.ijthermalsci.2008.02.009.
[27] Z. Anwar, B. Palm, R. Khodabandeh, Flow boiling heat transfer, pressure drop and dryout characteristics of R1234yf: experimental results and predictions, Exp. Thermal Fluid Sci. 66 (2015) 137–149, https://doi.org/10.1016/j.expthermflusci.2015.03.021.
[28] S.S. Bertsch, E.A. Groll, S.V. Garimella, Effects of heat flux, mass flux, vapor quality, and saturation temperature on flow boiling heat transfer in microchannels, Int. J. Multiphase Flow 35 (2009) 142–154, https://doi.org/10.1016/j.ijmultiphaseflow.2008.10.004.
[29] V. Dupont, J.R. Thome, A.M. Jacobi, Heat transfer model for evaporation in microchannels. Part II: comparison with the database, Int. J. Heat Mass Transf. 47 (2004) 3387–3401, https://doi.org/10.1016/j.ijheatmasstransfer.2004.01.007.
[30] C.B. Tibiriçá, G. Ribatski, Flow patterns and bubble departure fundamental characteristics during flow boiling in microscale channels, Exp. Thermal Fluid Sci. 59 (2014) 152–165, https://doi.org/10.1016/j.expthermflusci.2014.02.017.
[31] M.G. Cooper, Saturation nucleate Pool boiling - a simple correlation, Inst. Chem. Eng. Symp. Ser. (1984) 785–793, https://doi.org/10.1016/b978-0-85295-175-0.50013-8.
[32] S. Bortolin, A. Francescon, G. Ribatski, D. Del Col, Flow boiling of R134a and HFE-7000 in a single silicon microchannel with microstructured sidewalls, Int. J. Heat Mass Transf. 179 (2021) 121653, https://doi.org/10.1016/j.ijheatmasstransfer.2021.121653.
[33] L. Sun, K. Mishima, An evaluation of prediction methods for saturated flow boiling heat transfer in mini-channels, Int. J. Heat Mass Transf. 52 (2009) 5323–5329, https://doi.org/10.1016/j.ijheatmasstransfer.2009.06.041.
[34] G.M. Lazarek, S.H. Black, Evaporative heat transfer, pressure drop and critical heat flux in a SmallVertical TubeWith R-113, Int. J. Heat Mass Transf. 25 (1982) 945–960.
[35] K.E. Gungor, R.H.S. Winterton, General correlation for flow boiling in tubes and annuli, Int. J. Heat Mass Transf. 29 (1986) 351–358.
[36] S.S. Bertsch, E.A. Groll, S.V. Garimella, A composite heat transfer correlation for saturated flow boiling in small channels, Int. J. Heat Mass Transf. 52 (2009) 2110–2118, https://doi.org/10.1016/j.ijheatmasstransfer.2008.10.022.
[37] J.R. Thome, V. Dupont, A.M. Jacobi, Heat transfer model for evaporation in microchannels. Part I: presentation of the model, Int. J. Heat Mass Transf. 47 (2004) 3375–3385, https://doi.org/10.1016/j.ijheatmasstransfer.2004.01.006.
[38] J.C. Chen, A correlation for boiling heat transfer to saturated fluids in convective flow, Ind. Eng. Chem. Process. Des. Dev. 5 (1966) 322–329.
[39] M.G. Cooper, Heat flow rates in saturated nucleate Pool boiling-a wide-ranging examination using reduced properties, Adv. Heat Tran. 16 (1984) 157–239, https://doi.org/10.1016/S0065-2717(08)70205-3.
[40] J.R. Thome, Prediction of the mixture effect on boiling in vertical Thermosyphon reboilers, Heat Transf. Eng. 10 (2) (1989) 29–38.
[41] A. Cavallini, D. Del Col, L. Doretti, G.A. Longo, L. Rossetto, Refrigerant vaporization inside enhanced tubes: a heat transfer model, Heat Technol. 17 (1999) 29–36.
[42] K.J. Bell, M.A. Ghaly, An approximate generalized design method for multicomponent/partial condensers, AIChe. Symp. Ser. 69 (1973) 72–79.
[43] D. Del Col, M. Bortolato, S. Bortolin, Comprehensive experimental investigation of two-phase heat transfer and pressure drop with propane in a minichannel, Int. J. Refrig. 47 (2014) 66–84, https://doi.org/10.1016/j.ijrefrig.2014.08.002.
[44] D. Del Col, M. Azzolin, S. Bortolin, A. Berto, Experimental results and design procedures for minichannel condensers and evaporators using propylene, Int. J. Refrig. 83 (2017) 23–38, https://doi.org/10.1016/j.ijrefrig.2017.07.012.